HHS Public Access

Author manuscript

Mol Cell. Author manuscript; available in PMC 2019 October 18.

Published in final edited form as:

Mol Cell. 2018 October 18; 72(2): 286–302.e8. doi:10.1016/j.molcel.2018.08.022.

Release of ubiquitinated and non-ubiquitinated nascent chains from stalled mammalian ribosomal complexes by ANKZF1 and Ptrh1

Kazushige Kuroha[#1,#], **Alexandra Zinoviev**[#1], **Christopher U. T. Hellen**[1], and **Tatyana V. Pestova**[1,2,#]

[1]Department of Cell Biology, SUNY Downstate Medical Center, Brooklyn, NY, USA

[2]Lead contact

[#] These authors contributed equally to this work.

Abstract

The ribosome-associated quality control (RQC) pathway degrades nascent chains (NCs) arising from interrupted translation. First, recycling factors split stalled ribosomes, yielding NC-tRNA/60S ribosome-nascent chain complexes (60S RNCs). 60S RNCs associate with NEMF, which recruits the E3 ubiquitin ligase Listerin that ubiquitinates NCs. The mechanism of subsequent ribosomal release of Ub-NCs remains obscure. We found that in non-ubiquitinated 60S RNCs and 80S RNCs formed on non-stop mRNAs, tRNA is not firmly fixed in the P-site, which allows peptidyl-tRNA hydrolase Ptrh1 to cleave NC-tRNA, suggesting the existence of a pathway involving release of non-ubiquitinated NCs. Association with NEMF/Listerin and ubiquitination of NCs results in accommodation of NC-tRNA, rendering 60S RNCs resistant to Ptrh1 but susceptible to ANKZF1, which induces specific cleavage in the tRNA acceptor arm, releasing proteasome-degradable Ub-NCs linked to four 3'-terminal tRNA nucleotides. We also found that TCF25, a poorly characterized RQC component, ensures preferential formation of the K48-ubiquitin linkage.

Graphical Abstract

[#]**Corresponding authors**: Tatyana V. Pestova (Lead contact), Department of Cell Biology, SUNY Downstate Medical Center, 450 Clarkson Avenue, Box 44, Brooklyn, NY 11203, Phone: 718-270-1034, Fax: 718-270-2656, tatyana.pestova@downstate.edu, Kazushige Kuroha, Department of Cell Biology, SUNY Downstate Medical Center, 450 Clarkson Avenue, Box 44, Brooklyn, NY 11203, Phone: 718-270-1034, Fax: 718-270-2656, kazushige.kuroha@downstate.edu.

AUTHOR CONTRIBUTIONS

K.K. and A.Z. performed all experiments. T.V.P., K.K., A.Z., and C.U.T.H. designed the experiments and interpreted the data. T.V.P. wrote the paper with input from other authors.

DECLARATION OF INTERESTS

The authors declare no competing interests.

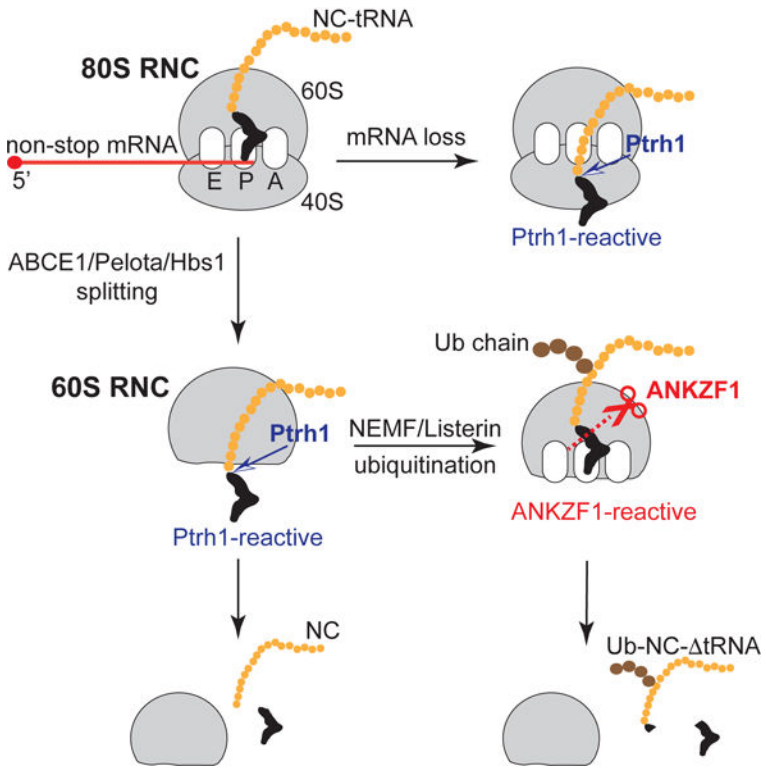

eTOC Blurb

Stalled ribosomes arising from interrupted translation are dissociated, after which tRNA-linked polypeptides associated with 60S subunits undergo ubiquitination. Subsequent ribosomal release of ubiquitinated polypeptides is mediated by ANKZF1. Kuroha et al. found that ANKZF1 induces specific cleavage in tRNA, releasing proteasome-degradable ubiquitinated polypeptides linked to four 3'-terminal tRNA nucleotides.

Keywords

ribosome-associated quality control; ANKZF1; Vms1; Ptrh1; TCF25; NEMF; Listerin; ubiquitination; proteasomal degradation

INTRODUCTION

Protein homeostasis prevents aberrant polypeptides from accumulating in cells, and defects in the quality control processes that monitor and degrade such polypeptides underlie neurodegenerative and other diseases (Balchin et al., 2016). The recently discovered ribosome-associated quality control (RQC) pathway detects truncated nascent chain (NC) polypeptides that might exert dominant negative effects, and targets them for proteasomal degradation (Brandman and Hegde, 2016). Such NCs arise from stalling of ribosomes on mRNAs due to e.g. lack of a stop codon or the presence of poly(A) sequences, multiple consecutive rare codons or stable secondary structures in the coding region (Inada, 2017).

The process is thought to initiate with the endonucleolytic cleavage of mRNA near the stall site followed by disassembly of elongation complexes. The nature of this cleavage and the factors responsible for it remain unknown, whereas disassembly of elongation complexes stalled at the 3'-end of the 5'-terminal mRNA cleavage fragment is mediated by ABCE1 in cooperation with Pelota and Hbs1 (Pisarev et al., 2010; Pisareva et al., 2011; Shao and Hegde, 2014). Pelota and Hbs1 are paralogues of eRF1 and eRF3, respectively, but unlike eRF1, Pelota does not induce peptide release, and ABCE1 therefore splits elongation complexes into 40S subunits, mRNA and NC-tRNA-associated 60S subunits. mRNA cleavage products are then degraded by Xrn1 and the RNA exosome, whereas the resulting NC-tRNA•60S ribosome-nascent chain complexes (60S RNCs) are recognized and processed by the RQC machinery, which includes the RING-type E3 ubiquitin (Ub) ligase Listerin (Ltn1 in yeast), NEMF (Rqc2 in yeast), TCF25 (Rqc1 in yeast), and the p97 (Cdc48 in yeast) ATPase with its Npl4 and Ufd1 cofactors (Brandman et al., 2012; Defenouillère et al., 2013; Brandman and Hegde, 2016). Thus, dissociation of the 40S subunit exposes the P site peptidyl-tRNA and intersubunit interface on the 60S subunit, allowing binding of NEMF which promotes recruitment of Listerin (Shao et al., 2015), which ubiquitinates 60S-associated NCs, targeting them for proteasomal degradation (Brandman et al., 2012; Shao et al., 2013).

Cryo-EM studies (Lyumkis et al., 2014; Shao et al., 2015; Shen et al., 2015) revealed that NEMF binds to tRNA and to the interface surface of the 60S subunit, preventing reassociation of a 40S subunit. Listerin binds to NEMF and to the 60S subunit, with its RING domain adjacent to the exit tunnel, poised to ubiquitinate the protruding NC within a small window (~12 amino acids) outside the exit tunnel (Kostova et al., 2017). In yeast, Rqc2 (NEMF) also recruits specific aminoacyl-tRNAs to the A site and promotes non-templated elongation of NCs by addition of carboxy-terminal Ala and Thr "CAT tails" (Shen et al., 2015), possibly to move the NC through the exit channel so that lysine residues that were shielded become accessible to Ltn1 (Kostova et al., 2017). The location of TCF25 on RNCs is unknown, and its function is poorly understood.

A prerequisite for proteasomal degradation of ubiquitinated NCs is their release from 60S subunits. Initial studies implicated p97 in this process. p97 is an abundant member of the AAA^+ (ATPase associated with diverse cellular activities) family of proteins. Each p97 monomer contains an N-terminal domain and two ATPase domains which form two stacked hexamers surrounding a central pore, and are responsible for p97's activity in remodeling ubiquitinated substrates (Bodnar and Rapoport, 2017). The intrinsic Ub-binding affinity of p97 is enhanced by Npl4 and Ufd1, which bind to the N domain. p97 binds to RNCs only after Listerin-mediated ubiquitination of NCs, and requires Rqc1 and Rqc2, although in what capacity is not known (Brandman et al., 2012; Defenouillère et al., 2013). The functions of p97 in RQC are thought to be to extract the ubiquitinated NC from the exit tunnel and to deliver it to the proteasome for degradation (Defenouillère et al., 2013; Verma et al., 2013). However, the attached tRNA moiety would be sterically unable to traverse the exit tunnel during this process, so that prior release of tRNA from the peptidyl-tRNA would undoubtedly be required.

Recent studies identified yeast Vms1 and its human homolog ANKZF1 as factors that release ubiquitinated NCs from 60S subunits (Verma et al., 2018; Zurita Rendón et al., 2018). Previously, Vms1 was found to displace Rqc2 from RNCs, antagonizing CAT-tailing, and is thought to prevent the import of defective, potentially toxic proteins into mitochondria (Izawa et al., 2017). Mammalian ANKZF1 contains an N-terminal leucine-rich sequence (LRS), a C2H2 zinc finger, a large mitochondrial targeting domain (MTD), two Ankyrin repeats, a coiled coil domain, a VCP-interacting motif (VIM) through which it binds to p97, and a C-terminal treble clef zinc finger that is absent in fungi (Heo et al., 2013; Nielson et al., 2017). Vms1 is primarily cytosolic due to inhibition of MTD function by its intermolecular sequestration by the LRS. In yeast, mitochondrial stress increases the mitochondrial abundance of ergosterol peroxide, and its binding to the MTD competitively displaces the LRS, causing Vms1 to relocate to mitochondria (Heo et al., 2010, 2013; Nielson et al., 2017). The Vms1 MTD adopts an RNase H-like fold composed of a β-sheet flanked by α-helices, and the observation that it is structurally related to the M domain of eRF1 (Nielson et al., 2017; Song et al., 2000) led to suggestions that it functions as an eRF1-like inducer of peptidyl-tRNA hydrolysis in the PTC of RNCs (Verma et al., 2018; Zurita Rendón et al., 2018). However, although ANKZF1/Vms1 contains a conserved glutamine residue that is proposed to function analogously to the same residue in the GGQ motifs of eukaryotic eRF1 and prokaryotic RF1/RF2, they do not contain two essential preceding Gly residues (the suggested equivalent motif in human ANKZF1 is $TAQ_{244–6}$), which raises doubts about this assignment.

Here, we reconstituted the mammalian RQC pathway *in vitro*, from stalling of ribosomes to recognition and processing of 60S RNCs by the RQC machinery and degradation of ubiquitinated NCs by the 26S proteasome. We report that ANKZF1 does not function as a peptidyl-tRNA hydrolase. Instead, it induces specific cleavage in the acceptor arm of 60S-bound P site tRNA releasing proteasome-degradable NCs linked to a 4nt-long 3’terminal portion of tRNA. We also identified an important role of Ptrh1 in release of non-ubiquitinated NCs from 60S RNCs and 80S stalled ribosomes, and found that TCF25 promotes preferential formation of the K48 Ub linkage during Listerin-mediated ubiquitination.

RESULTS

Ptrh1 promotes release of non-ubiquitinated NCs from 60S and 80S RNCs

To investigate NC release, we used a β-VHP construct (Shao et al., 2013) containing the coding region for the short structured villin headpiece (VHP; McKnight et al., 1996) and an unstructured region from Sec61β ending with Val, followed by a stop codon and restriction sites to synthesize mRNA with/without a stop codon and 3’UTRs of different lengths (Figure 1A). Translation of these mRNAs yields 80S RNCs containing a tightly folded protein domain outside the exit tunnel tethered to P site tRNA by an unstructured linker. 60S RNCs obtained after splitting of such 80S RNCs have minimal NC-tRNA drop-off and are ideal substrates for studying RQC (Shao et al., 2013). The presence at the end of NC-tRNA of Val-$tRNA^{Val}$, whose ester bond is exceptionally resistant to spontaneous hydrolysis

(Hentzen et al., 1972), ensures NC-tRNA integrity during sample preparation and SDS-PAGE (Shao et al., 2013).

Consistent with the weak ubiquitination pathway in rabbit reticulocyte lysate (RRL) (Shao et al., 2013), translation of non-stop β-VHP mRNAs yielded non-ubiquitinated products, but despite the stability of Val-tRNA^{Val}, a large proportion of β-VHP was released from tRNA (shown for β-VHP(+2) mRNA, with 2 nts after the last codon: Figure 1B, lanes 1–6). In control experiments, translation of mRNAs containing stop codons yielded predominantly free β-VHP (Figure 1B, lanes 7–18).

To investigate the mechanism of β-VHP release during translation of non-stop mRNAs, we isolated the releasing activity using 60S RNCs as the substrate and monitoring release by SDS-PAGE. To obtain 60S RNCs, 80S RNCs were formed by translating non-stop mRNA in RRL, purified by sucrose density gradient (SDG) centrifugation (Figure S1A), and split by ABCE1/Pelota/Hbs1. The resulting 60S RNCs were isolated by a second round of centrifugation (Figure S1A). Small amounts of “native” 60S RNCs detected during the first round were also purified further by the second round. After two rounds of centrifugation, “native” 60S RNCs did not contain associated NEMF/Listerin, which was confirmed by mass spectrometry and ubiquitination assay (not shown), and therefore “native” 60S RNCs and those obtained by splitting 80S RNCs behaved identically in all assays. We note that the 60S RNC peak overlaps partially with the 80S RNC peak after SDG centrifugation, and since both peaks are very similar in size (e.g. Figure S1A, right panel), purified 60S RNCs contain low amounts of contaminating 80S RNCs.

Initial purification from RRL identified two activities: one generated free β-VHP (Figure 1C) and the other, β-VHP linked to a tRNA fragment, which was confirmed by treatment of the product with RNase A (Figures 1D, S1B). Isolation of the first activity from HeLa cells (Figure 1E) yielded Ptrh1 (Table S1), a putative peptidyl-tRNA hydrolase homologous to bacterial peptidyl-tRNA hydrolase Pth (Figure S1C). The second activity was identified as Slfn14 (Pisareva et al., 2015) (Figure 1E; Table S2).

Recombinant Ptrh1 (Figure 1F) released β-VHP from 60S RNCs and hydrolyzed free β-VHP-tRNA, but strikingly, also released β-VHP from 80S RNCs formed on non-stop mRNAs (Figure 1G). H46N and D121A substitutions, corresponding to essential residues in Pth (Figure S1C; Schmitt et al., 1997), abolished Ptrh1’s activity on all substrates (Figure 1G), suggesting a conserved mechanism of release. In SDG centrifugation experiments, incubation of RNCs without Ptrh1 did not affect their integrity (Figure 1H). Ptrh1-mediated release was therefore not preceded by RNC dissociation. Ptrh1 was active over a wide [Mg^{2+}] range (Figure S1D), and hydrolyzed all substrates at similar rates, with a slight preference for 60S RNCs (Figure 1I). Slfn14 also hydrolyzed β-VHP-tRNA in 60S and 80S RNCs, but much more slowly (Figure S1E).

In RRL, addition of Ptrh1 during translation of non-stop mRNA induced complete release of β-VHP (Figure S1F), suggesting that the endogenous Ptrh1 level is low. Slfn14 did not affect β-VHP release (Figure S1G) and was not studied further.

Determinants of Ptrh1 specificity for 80S RNCs

To establish determinants of Ptrh1 specificity for 80S RNCs, we first prepared RNCs with >2 mRNA nts after the P site by translating mRNAs with stop codons and defined 3'UTRs in the presence of $eRF1^{AGQ}$ mutant, which arrests translation at the pre-termination stage. SDG centrifugation dissociates $eRF1^{AGQ}$, yielding factor-free 80S RNCs (Zinoviev et al., 2015). Ptrh1 retained some activity on 80S RNCs with 3 nts after the P site, but was inactive on complexes with ≥9 nts (Figure 2A).

To assay the importance of tRNA identity, non-stop β-VHP mRNA with a 3'-terminal Ser codon was translated in the presence of Ser-[^{32}P]$tRNA^{Ser}$. The resulting 80S RNCs were fully susceptible to Ptrh1 (Figure 2B). Similar results were obtained for 80S RNCs containing $tRNA^{Cys}$ (not shown). Analysis of 80S RNCs containing NCs in which unstructured linkers had been placed in the Sec61β region to move the VHP domain out of the exit tunnel showed that VHP folding does not influence Ptrh1's activity (Figure 2C). Ptrh1 also released NCs that are unrelated to β-VHP (Figure 2D).

NC length strongly modulated Ptrh1 activity (Figure 2E, left panel). Hydrolysis did not occur on RNCs containing 14–55 aa-long NCs (Figure 2E, middle panels), and Ptrh1 acted on them only after splitting by ABCE1/Pelota/Hbs1 (Figure 2F). Ptrh1 was also not active on RNCs with very short NCs (4– 6 aa), irrespective of whether they formed in RRL or were reconstituted *in vitro* (Figures S2A-B). In contrast, Ptrh1 efficiently released 75 and 66 aa-long NCs (Figure 2E, right panel).

In conclusion, Ptrh1 released NCs from 80S RNCs containing sufficiently long NCs and <3 mRNA nts downstream from the P site. Notably, its activity was unaffected by A or E site ligands (Figures S2C-E).

The ability to release NCs from 60S/80S complexes was not unique to Ptrh1. Bacterial Pth and mitochondrial Ptrh2 belonging to a different peptidyl-hydrolase class (de Pereda et. al, 2004) also released NCs from 60S/80S complexes and had the same dependence on the number of mRNA nts after the P site and the length of NCs in 80S RNCs (Figure S3). In contrast, the mitochondrial factor ICT1 containing a GGQ motif (Akabane et al., 2014) and the putative peptidyl-tRNA hydrolase PtrhD1 (Burks et al., 2016) were not active in these assays.

Strikingly, Ptrh1 and puromycin showed opposite 80S RNC substrate specificities. Puromycin acted poorly or not at all on complexes with long NCs and < 3 mRNA nts after the P site (Figures 2G-H). Addition of puromycin to RRL following translation of non-stop mRNA also did not lead to β-VHP release (Figure 2I). However, puromycin was active on 80S RNCs with short NCs or long 3'-terminal mRNA regions (Figure 2J). In some 80S RNCs formed on non-stop mRNAs, complete release occurred only with both Ptrh1 and puromycin (Figure 2K).

The fact that 80S RNCs that are Ptrh1-susceptible do not react with puromycin suggests that the CCA end of their peptidyl-tRNA is not accommodated in the peptidyl transferase center (PTC). The lack of effect of A and E site ligands on Ptrh1-mediated hydrolysis and the

similar activities of peptidyl-hydrolases from unrelated classes also suggest that Ptrh1 acts on 80S RNCs in which tRNAs do not interact intimately with ribosomes and are flexibly attached to them via NCs.

In conclusion, our data suggest the existence of a pathway that involves Ptrh1-mediated release of non-ubiquitinated NCs.

Ubiquitination of 60S RNCs: the role of TCF25

To investigate release of Ub-NCs, ubiquitination was reconstituted *in vitro*. β-VHP contains 8 lysines (Figure S4A), and if Listerin monitors a window outside the exit tunnel like Ltn1 (Kostova et al., 2017), ubiquitination of K55/K70 would be expected. Recombinant NEMF, Listerin, TCF25, p97, Npl4 and Ufd1 were purified for these experiments (Figure 3A), and p97's ATPase activity was confirmed (Figure S4B). Consistent with previous reports (Shao et al., 2013; 2015), ubiquitination of 60S RNCs occurred in the presence of Listerin, Ube1, Ube2D1 and *wt* Ub, and was stimulated by NEMF, particularly at low Listerin concentrations (Figure 3B). In this and other experiments described below, low levels of β-VHP that could not be ubiquitinated were engaged with the contaminating 80S RNCs present in preparations of 60S RNCs. p97 did not influence ubiquitination, and Ufd1-Npl4 only slightly decreased the molecular weights of Ub-products (Figures 3C-D, lanes 1–3). In contrast, TCF25 substantially reduced the size of Ub chains, particularly in the presence of NEMF (Figures 3C-D, lanes 4).

Ube2D family E2s are indiscriminate, and with RING-type E3s promote transfer of Ub to any of seven lysines, yielding non-degradable forked Ub chains (Stewart et al., 2016). Given that non-stop mRNA translation products are degraded by the proteasome pathway, we investigated the influence of TCF25 on Listerin/Ube2D1-mediated synthesis of homogenous K48 chains using K48 single-Lys mutant Ub. In contrast to ubiquitination by *wt* Ub, K48-specific ubiquitination was not inhibited by TCF25 (Figure 3C, compare lanes 7 and 10). Moreover, in the absence of NEMF, TCF25 strongly stimulated K48-specific ubiquitination (Figure 3D, compare lanes 7 and 10), which was otherwise inefficient compared to *wt* Ub.

Next, we assayed TCF25's influence on other linkages. Listerin/NEMF/Ube2D1 could form all linkages, but the longest chains were obtained with K6, K11, K33 and K63 single-Lys mutants (Figure 3E, lanes 5, 7, 13 and 15). Strikingly, TCF25 inhibited synthesis of all these linkages, as well as ubiquitination by K48R and K29R/K48R/K63R Ub (Figure 3E). Qualitatively similar effects occurred in the absence of NEMF (Figure S4C). Thus, in the case of the Ube2D1/Listerin pair, TCF25 specifically stimulated K48 ubiquitination and inhibited all others.

Next, we investigated whether TCF25 has the same effect if Listerin is paired with other E2s. As noted (Shao et al., 2013), ubiquitination was most efficient when Listerin was combined with Ube2D family E2s (Figure 3F). Although Ube2E1, Ube2E3, Ube2K, and Ube2N/V1 and Ube2N/V2 heterodimers also synthesized relatively long Ub chains, their activities were lower to varying degrees. Ube2F, Ube2J2 and Ube2W2 attached only a few Ub molecules, whereas other tested E2s were inactive. Ubiquitination by all E2s was strictly Listerin-dependent (Figure S4D).

As in the case of Ube2D1, TCF25 also strongly stimulated K48 ubiquitination by other Ube2D family members and slightly inhibited ubiquitination with *wt* Ub (Figure 3G, lanes 1–6). For Ube2E family E2s, stimulation was observed for both *wt* and K48 Ub (Figure 3G, lanes 7–10). No significant changes occurred during ubiquitination by Ube2K, Ube2N/V1 and Ube2N/V2 (Figure 3G, lanes 11–16). TCF25 had qualitatively similar effects in NEMF's absence (Figure S4E).

Analysis of other linkages revealed that Ube2D2 and Ube2D3 formed relatively long chains with K11-Ub, but as with Ube2D1, this was inhibited by TCF25 (Figure 3H, lanes 9–10). Some stimulation by TCF25 was observed for K63-Ub (Figure 3H, lanes 19–20), but the strongest response and the highest ubiquitination occurred with K48-Ub (Figure 3H, lanes 17–18). As with Ube2D1, TCF25 inhibited ubiquitination by Ube2D2 and Ube2D3 with K48R and K29R/K48R/K63R Ub (Figure 3H, lanes 3–6). Ube2E family E2s formed long Ub chains only with the K11-Ub, which was also inhibited by TCF25, as was ubiquitination with K48R and K29R/K48R/K63R Ub (Figure 3I, lanes 3–6 and 9–10). Stimulation was observed for K48-Ub, and to lesser extent, K63-Ub (Figure 3I, lanes 17–20), but the overall stimulatory effect was lower than for Ube2D family E2s. Thus, TCF25 elicited its strongest effect when Listerin was paired with Ube2D family E2s.

Analysis of TCF25's influence when Ube2D3 or Ube2D1 were combined with Mdm2, a different RING-type E3 ligase, showed that it did not affect ubiquitination of S5a or p53 (Figures 3J-K and not shown). Thus, TCF25's effect was specific for Ube2D/Listerin pairs.

To confirm that TCF25 promotes preferential formation of K48 linkage during ubiquitination with *wt* Ub, 60S RNCs ubiquitinated by Listerin/Ube2D with or without TCF25 were treated by deubiquitinating enzymes with different specificities (Figure 3L). TCF25 did not affect deubiquitination by Usp2, which can process all Ub linkages (Ye et al., 2011), increased deubiquitination by Otub1, which is K48-specific (Edelmann et al., 2009), but impaired the activity of Yod1 which preferentially hydrolyzes K11, K27, K29 and K33 linkages (Mevissen et al., 2013).

Ptrh1 does not promote release of ubiquitinated NCs

NEMF, particularly with Listerin, moderately inhibited Ptrh1-mediated release of non-ubiquitinated β-VHP from 60S RNCs (Figures 4A and S5A). In ubiquitination conditions, Ptrh1 released only low-ubiquitinated NCs obtained with Listerin alone (evident by the increased mobility of Ub-products), but did not hydrolyze highly-ubiquitinated NCs obtained with or without NEMF (Figure 4B). β-VHP-tRNA, which was not ubiquitinated and was hydrolyzed by Ptrh1, was engaged into 80S RNCs that were present in small quantities in preparations of 60S RNCs. SDG centrifugation experiments confirmed that Ptrh1 released only low-ubiquitinated β-VHP formed with Listerin alone (Figure 4C). Ptrh1 regained full activity after deubiquitination of SDG-purified ubiquitinated 60S RNCs (Figure S5B). These results argue against Ptrh1's involvement in RQC.

In contrast, delayed addition of puromycin to ubiquitination reactions or to S DG-purified ubiquitinated 60S RNCs reduced the molecular weights of Ub-products, suggesting that it released Ub-NCs (Figure 4D-E). Interestingly, inclusion of puromycin from the start of

ubiquitination led to shorter Ub-products if reaction mixtures lacked TCF25, suggesting that it also accelerates ubiquitination (Figure S5C). Puromycin-induced release of Ub-NCs was confirmed by SDG centrifugation experiments (Figure 4F). NEMF/Listerin also increased the susceptibility to puromycin of non-ubiquitinated 60S RNCs (Figure S5D). Thus, association with NEMF/Listerin and ubiquitination of 60S RNCs led to accommodation of NC-tRNA in the PTC, rendering RNCs puromycin-reactive but resistant to Ptrh1.

The end-point in RQC is proteasomal degradation of Ub-NCs. In addition to Ub chains, it requires the presence in substrates of a ~30 aa-long unstructured region (Yu et al., 2016). In 60S-bound β-VHP, the unstructured C-terminal region is sequestered in the exit tunnel. Consistently, 26S proteasome did not degrade 60S-bound Ub-β-VHPs, even though they were ubiquitinated with *wt* or K48 Ub in the presence of TCF25, which even with *wt* Ub ensures preferential formation of the Lys^{48} linkage that marks polypeptides for proteasomal degradation (Figure 5A). The process was not stimulated by p97/Ufd1-Npl4 with/without Yod1, a mammalian homologue of yeast deubiquitinase Otu1 involved in Cdc48-dependent reactions (Bodnar and Rapoport, 2017) (Figure 5A), or by inclusion into ubiquitination mixtures of S5a, which inhibits formation of non-degradable forked Ub chains (Kim et al., 2009) (Figure S5E).

Proteasomal degradation of Ub-β-VHP depended on its release from 60S RNCs. Thus, degradation of highly ubiquitinated β-VHP occurred exclusively in the presence of puromycin (Figure 5B, lanes 8–9), whereas Ptrh1 stimulated degradation of only low- and non-ubiquitinated β-VHP (Figure 5B, lanes 14–15; Figure 5C). Degradation was not induced by total (Σ) deacylated tRNA, ICT1 or eRF1 (with/without eRF3 or ABCE1) (Figure S5F). p97/Ufd1-Npl4 with/without Yod1 did not influence puromycin-dependent degradation in time course experiments (Figure S5G).

To determine whether 26S proteasomes can degrade 60S-bound Ub-NCs if they have exposed unstructured regions, 35–54 aa-long Sec61β fragments were placed at the N-terminus of β-VHP (35– 54aa+β-VHPs; Figure 5D). Although proteasomes could degrade Ub-35–54aa+β-VHPs without their prior release by puromycin, this was less efficient and yielded a distinct identical product that migrated faster than NC-tRNAs and could be hydrolyzed by Ptrh1 (Figure 5E), suggesting that it comprised tRNA linked to a portion of β-VHP that was protected by the 60S subunit (Δβ-VHP-tRNA). However, Δβ-VHP-tRNA did not accumulate at any point during degradation of purified 60S-bound Ub-35aa+β-VHPs in the HeLa cell extract (Figure 5F), indicating the existence of a factor promoting release of Ub-NCs.

ANKZF1-mediated release of ubiquitinated NCs from 60S RNCs

Two recent studies identified yeast Vms1 and its human homolog ANKZF1 as release factors for ubiquitinated NCs (Verma et al., 2018; Zurita Rendón et al., 2018). The structural similarity of the MTD to the RNase H fold of the eRF1 M domain (Nielson et al., 2017) led to the suggestion that Vms1 and ANKZF1 function similarly to eRF1, inducing hydrolysis of the NC-tRNA ester bond.

Incubation of recombinant human ANKZF1 (Figure 6A) with SDG-purified ubiquitinated 60S RNCs led to release of Ub-[^{35}S]β-VHP (Figure 6B), which allowed its subsequent degradation by 26S proteasomes (Figure 6C). Degradation was slightly stimulated by p97/Ufd1-Npl4 and moderately inhibited by NEMF/Listerin. Degradation in the presence of both sets of factors was weaker than in their absence, but higher than in the presence of only NEMF/Listerin, indicating that their negative effect was partially offset by p97/Ufd1-Npl4.

In experiments with non-ubiquitinated 60S RNCs, ANKZF1 alone, or with Listerin or p97/Ufd1-Npl4 resulted in the appearance of a faint band that migrated slightly more slowly than free β-VHP (Figure 6D, lanes 1–4). Strikingly, incubation of 60S RNCs with ANKZF1 and NEMF yielded a very prominent band corresponding to β-VHP linked to a short tRNA^{Val} fragment (Figure 6D, lanes 5–8), the presence of which was confirmed by its removal by delayed addition of RNase A (Figure 6D, lanes 9 and 10). In time course experiments, p97/Ufd1-Npl4 and Listerin only marginally stimulated NEMF-dependent release of β-VHP-ΔtRNA^{Val} by ANKZF1 (Figure 6E). ANKZF1 also induced NC-ΔtRNA release from 60S RNCs containing NCs and tRNAs other than β-VHP and tRNA^{Val} (Figure S6A), indicating that the nature of tRNA and NC was not critical. Importantly, ANKZF1 did not induce NC-ΔtRNA release in 80S RNCs assembled on non-stop mRNAs irrespective of whether they were susceptible to Ptrh1 or puromycin, or in 80S pre-termination complexes assembled on mRNA with a stop codon and a short 3'UTR (Figure 6F).

Thus, although NEMF slightly inhibited ANKZF1-mediated release of Ub-NCs from SDG-purified 60S RNCs, it was required for ANKZF1-mediated hydrolysis of NC-tRNA in non-ubiquitinated 60S RNCs. This apparent contradiction can be explained by the difference in tRNA positions in both complexes. In non-ubiquitinated 60S RNCs, tRNA accommodates in the P site only in the presence of NEMF, whereas in ubiquitinated complexes, ubiquitination of NCs maintains tRNA in the accommodated position even if NEMF/Listerin dissociate during centrifugation. Thus, NEMF ensures tRNA accommodation, which is required for ANKZF1-mediated cleavage of tRNA, but at the same time, it may also delay tRNA cleavage to allow sufficient ubiquitination to occur, given that ANKZF1, as expected, inhibited ubiquitination (Figure 6G).

In SDG centrifugation experiments, ANKZF1 and NEMF bound individually to free 60S subunits but not to 80S ribosomes (Figure 6H). Their binding to 60S subunits may be weakly cooperative, because their levels in 60S fractions were slightly higher when they were both present in reaction mixtures. In electrophoretic mobility shift assays (EMSA), ANKZF1 and NEMF also bound to tRNA^{Val} and tRNA^{Ser}, but a super-shift in the presence of both proteins was not observed, suggesting that they did not bind to the same tRNA molecule (Figure 6I). Although ANKZF1 bound to individual tRNA^{Val}, it did not cleave free β-VHP-tRNA^{Val} (Figure S6B).

To determine the fate of the entire tRNA during ANKZF1-mediated release of NC-ΔtRNA, we prepared 60S RNCs containing [^{32}P]tRNA by translating β-VHP mRNA in the presence of Val-[^{32}P]tRNA^{Val}. SDS-PAGE analysis showed that Ptrh1 released intact tRNA^{Val} from 60S RNCs (Figure 7A, lane 3), whereas Slfn14 yielded [^{32}P]-labeled β-VHP-ΔtRNA, but the rest of tRNA was degraded (Figure 7A, lane 4). In contrast to Slfn14, ANKZF1 did not

hydrolyze tRNA completely, but only slightly shortened it, yielding a distinct truncated fragment (Figure 7A, lane 2). ANKZF1 also did not show non-specific nuclease activity and did not hydrolyze free tRNAs or mRNAs (Figure S6C). Importantly, ANKZF1-mediated release of Ub-NCs from ubiquitinated 60S RNCs also occurs via tRNA cleavage. Thus, ANKZF1 promoted shortening of tRNA in ubiquitinated 60S RNCs, and moreover, irrespective of whether they were ubiquitinated by Listerin/NEMF or by Listerin alone, even though Listerin did not stimulate cleavage in non-ubiquitinated 60S complexes (Figure 7B). These results again support the conclusion that accommodation of the P site tRNA is a prerequisite for its cleavage by ANKZF1, and it is not important whether it is achieved by interaction of 60S RNCs with NEMF or by ubiquitination of NCs.

To map the site of ANKZF1-mediated tRNA cleavage, 60S RNCs were formed on *wt* or mutant β-VHP mRNA containing Ser as the last codon, in the presence of Val-[^{32}P]tRNA^{Val} or Ser-[^{32}P]tRNA^{Ser}, respectively. 60S RNCs were then treated by Ptrh1 or ANKZF1 with or without prior ubiquitination, and the length of the tRNA fragments was determined in a sequencing gel. Irrespective of the ubiquitination status of 60S RNCs, ANKZF1 shortened both tRNA^{Ser} and tRNA^{Val} by 4 nucleotides, determined by comparing their mobility with the mobility of DNA fragments (Figure 7C) or a tRNA^{Val} ladder (Figure S6D).

The ANKZF1 mutant containing a TAQ→TAL substitution in the TAQ$_{244–6}$ motif did not induce tRNA cleavage in 60S RNCs containing β-VHP-tRNA^{Val} and did not stimulate 26S proteasomal degradation of Ub-β-VHP in SDG-purified ubiquitinated 60S RNCs (Figure 7D), confirming direct correlation between ANKZF1's nuclease activity and its ability to stimulate degradation. In contrast, a TAQ→GGQ mutant was active in both assays, continuing to cleave tRNA rather than hydrolyze the tRNA-NC ester bond (Figure 7D).

Interestingly, when analyzing whether ANKZF1's activity can be inhibited by addition of tRNA, which could potentially compete with ANKZF1 for binding to 60S RNCs, we found that incubation of 60S RNCs containing β-VHP-[^{32}P]tRNA^{Val} with NEMF and Σaa-tRNA (but not deacylated tRNA) led to tRNA^{Val} release (Figure 7E). When assayed using 60S RNCs containing [^{35}S]β-VHP-tRNA^{Val}, Σaa-tRNA promoted release of β-VHP that had a slightly lower mobility (Figure 7F). Release was enhanced by Listerin but was not affected by eEF2 (Figure 7G). However, when assayed by SDG centrifugation, NEMF and Σaa-tRNA did not decrease β-VHP's association with 60S RNCs (not shown), which suggests that release of [^{35}S]β-VHP observed by SDS-PAGE could be caused by electrophoretic conditions if NEMF had promoted addition of an aa-tRNA with a more labile ester bond than that of Val-tRNA^{Val}. Thus, it is possible that NEMF might also promote C-terminal extension of NCs.

In conclusion, ANKZF1 induces specific tRNA cleavage in ubiquitinated 60S RNCs, releasing proteasome-degradable Ub-NCs connected to a short (4 nt) 3'-terminal tRNA fragment.

DISCUSSION

Release of nascent chains from aberrant NC-tRNA•60S complexes arising from interrupted translation is a prerequisite for their subsequent degradation and is therefore a key step in the RQC pathway. Here we report that ubiquitinated and non-ubiquitinated NCs are released from 60S subunits by ANKZF1 and Ptrh1, respectively, but the mode of release and the composition of released products differ fundamentally. Thus, non-ubiquitinated NCs are released in the free form following Ptrh1-mediated hydrolysis of the NC-tRNA ester bond, whereas released ubiquitinated NCs remain linked to four 3'-terminal tRNA nucleotides following ANKZF1-induced specific cleavage in the acceptor arm of the P site tRNA.

Ptrh1-mediated release of non-ubiquitinated NCs

Ptrh1 released non-ubiquitinated NCs from 60S RNCs and also 80S RNCs formed on non-stop mRNAs and containing sufficiently long NCs. Neither complex was puromycin-sensitive, indicating that their tRNAs are not accommodated in the P site and are instead flexibly attached to ribosomes via NCs, allowing Ptrh1 to bind tRNA and hydrolyze the ester bond. The loose attachment of tRNA in 80S RNCs formed on non-stop mRNAs is most likely caused by the partial occupancy of the mRNA-binding channel. We cannot exclude that mRNA might even dissociate from such complexes and can also not exclude the possibility that cellular factors might enhance loosening of tRNA, since we are currently unable to reconstitute *in vitro* RNCs with sufficiently long NCs. Thus, it has been suggested that ribosomes reaching the end of non-stop mRNA are efficiently split with endogenous recycling factors but appear to reassociate rapidly (Shao et al., 2013), in which case mRNA would be released during dissociation, and reassociated 80S complexes would lack mRNA. Importantly, Ptrh1 activity on 80S RNCs was not an artifact of complex preparation, because addition of puromycin to RRL following translation of non-stop mRNAs did not affect NC-tRNA integrity, whereas addition of Ptrh1 led to NC release. One very probable reason why Ptrh1 is not active on 80S RNCs with short NCs is that the loss of the intimate contact between tRNA and the ribosome would result in NC-tRNA drop-off if NCs are short, in which case we may purify only the population of 80S RNCs with tRNA properly accommodated in the P site.

In what circumstances could Ptrh1-mediated release of non-ubiquitinated NCs be employed in cells? An obvious situation is when 60S RNCs cannot be ubiquitinated by Listerin because the NC in the Listerin-accessible 'window' lacks Lys residues (Kostova et al., 2017). In yeast, this problem can to some extent be overcome by CAT-tailing (Shen et al., 2015). Although our data suggest that NEMF-dependent addition of at least one amino acid may occur in mammalian 60S RNCs, long amino acid extensions did not form. Moreover, CAT-tailing will not solve the problem if there are no Lys residues hidden in the exit tunnel. In turn, Ptrh1-mediated NC release from 80S RNCs could be utilized if Pelota/Hbs1/ABCE1 activity is impaired or insufficient due to excessive accumulation of stalled 80S RNCs. Generally, the probability of Ptrh1-mediated release of non-ubiquitinated NCs from 80S and 60S RNCs in cells will be determined by the relative activities of Ptrh1, Pelota/Hbs1/ABCE1 and NEMF/Listerin. Notably, a role in rescue of stalled ribosomes has also been proposed for bacterial Pth (Vivanco-Domínguez et al., 2012).

ANKZF1-mediated release of ubiquitinated NCs

Fixation of tRNA in the P site following association of 60S RNCs with NEMF/Listerin and ubiquitination of NCs renders RNCs resistant to Ptrh1 but susceptible to tRNA cleavage by ANKZF1. This activity is consistent with recent reports that identified ANKZF1 and Vms1 as release factors (Verma et al., 2018; Zurita Rendón et al., 2018). However, it suggested (but did not prove) that ANKZF1 and Vms1 induce peptidyl-tRNA hydrolysis whereas we showed that ANKZF1 is an RNA endonuclease. Its activity is not restricted to specific tRNAs in 60S RNCs, but does require that peptidyl-tRNA is bound to the 60S subunit, with the tRNA moiety accommodated in the P site. Structural modeling (Figure S7) indicates that ANKZF1's MTD resembles Vms1 (Nielson et al., 2017) and is thus related to the RNAse H fold (β1β2β3α1β4α2β5α3) of the eRF1 M domain (Song et al., 2000). The essential element of eRF1 is the universally conserved GGQ motif in the β3-α1 loop. The Gly residues adopt a specific backbone conformation that cannot be achieved by any other amino acid, which allows placement of the GGQ motif into the PTC, enabling access of a water molecule and thus exposing the peptidyl-tRNA ester bond to nucleophilic attack (e.g. Jin et al., 2010). The conserved Gln coordinates a water molecule during hydrolysis. The two Gly residues are essential, and in prokaryotes, their mutation has an even more drastic effect than mutation of Gln (Shaw and Green, 2007). Athough ANKZF1 and Vms1 have a conserved Gln in the β3-α1 loop that is essential for activity (Verma et al., 2018; Zurita Rendón et al., 2018; this study), it is not preceded by Gly residues, which is inconsistent with ANKZF1 being an eRF1-like release factor.

The RNase H-like superfamily of proteins is involved in various processes, including DNA replication and repair, transposition and RNA interference. RNase H-like nucleases primarily cleave RNA endonucleoytically in RNA/DNA hybrids, but a subset can cleave dsRNA (Ohtani et al., 2004; Miyoshi et al., 2005). RNase H-like enzymes share a common mechanism of catalysis, in which two metal ions are jointly coordinated by the scissile phosphate and two active site carboxylates, bisecting the scissile phosphate (Majorek et al., 2014). The four catalytic Glu/Asp residues in β1, α1, β4 and α3 are generally but not universally conserved. However, we could not identify conserved candidate Glu/Asp residues in ANKZF1/Vms1 that could function in canonical RNase H-like two ion-dependent catalysis, suggesting that other, potentially flexible components of the MTD may contain determinants of ANKZF1's enzymatic activity. In this respect, we note that the β3-α1 loop is larger than in eRF1, contains highly conserved elements (Figure S7) and although its structure is not known, may form a small helix. Accordingly, determination of the structure of the ANKZF1/60S RNC complex by cryoEM is an important priority, to identify induced conformational changes in ANKZF1 and to gain insights into interactions and possible functions of peripheral domains.

The mechanism of function of ANKZF1 in the eukaryotic RQC pathway differs from the mechanisms of analogous processes in prokaryotes. ArfA recruits the canonical termination factor RF2 to stalled ribosomal complexes to catalyze peptidyl-tRNA hydrolysis, whereas ArfB, which has an N-terminal domain that is related to domain 3 of RF1 and RF2 (and like them contains an essential GGQ motif) binds to ribosomal complexes containing truncated mRNAs so that the GGQ motif is positioned at the PTC (Huter et al., 2017). Some bacteria

encode endonucleases that cleave in the acceptor stem of specific tRNAs (Morse et al., 2012), but there is no evidence that they are involved in rescue of stalled ribosomes. Consequently, the mechanism described here appears to establish a new paradigm.

Imposition by TCF25 of K48-specificity on ubiquitination by Listerin

A further important finding concerns the function of TCF25, a poorly characterized component of the RQC pathway. In yeast, Rqc1 was initially suggested to act downstream of ubiquitination by promoting recruitment of Cdc48/p97 to ubiquitinated 60S RNCs (Brandman et al., 2012; Defenouillère et al., 2013), but more recently was found to increase the rate of ubiquitination in a yeast cell-free system (Osuna et al., 2017). However, in biochemical experiments, TCF25 did not associate with NEMF/Listerin-bound 60S RNCs and did not stimulate ubiquitination (Shao et al., 2015). We found that TCF25 specifically stimulated formation of K48 ubiquitin linkages and inhibited all others. This finding accounts for observations that Listerin-mediated ubiquitination in RRL is K48-specific (Shao et al., 2013) and depletion of Listerin in HEK293T cells did not affect formation of K11/K48-branched chains (Yau et al., 2017) even though Listerin can, with several E2s, form Ub chains with all linkages in the *in vitro* reconstituted system, including long K11 chains (Figure 3).

Listerin is a RING-type E3 ligase. In contrast to HECT-type E3s that form an intermediate with ubiquitin before its transfer to the substrate and therefore determine Ub linkage specificity, RING-type E3s mediate the transfer of ubiquitin directly from E2~Ub to the substrate, in which case the specificity of linkage is determined by the E2, and a given RING-type E3 can generate different linkages depending on its E2 partner (Stewart et al., 2016). Although Listerin could function with Ube2K, which contains a unique region that interacts with Y59 near Ub-K48 and thereby ensures Ube2K's K48-linkage specificity (Middleton and Day, 2015), it also synthesized long Ub chains with Ube2E family E2s. Moreover, ubiquitination was most efficient when Listerin was combined with Ube2D family E2s that are known for their promiscuity (Stewart et al., 2016), implying that they can bind the acceptor ubiquitin at different sites and/or orientations (Middleton et al., 2017). TCF25 stimulated K48-specific ubiquitination when Listerin was combined with the Ube2E1 or Ube2E3, but its strongest effect was observed when Listerin was paired with Ube2D family E2s. In the only example characterized to date in which a separate protein influences E2 specificity, K63-specific linkage by Ube2N is determined by a non-catalytic E2-like co-factor, Ube2V1 or Ube2V2, that forms a heterodimer with the cognate E2, binds the acceptor Ub and positions its K63 residue close to the E2 active site (Eddins et al., 2006). Although TCF25 must function to orient ubiquitin such that K48 is positioned to attack the thioester bond of the E2-conjugated donor ubiquitin, TCF25 is not known to bind any E2. Moreover, the effect of TCF25 was Listerin-specific, and it did not influence the specificity of ubiquitination when Ube2D E2 was combined with the Mdm2 E3 ligase. Although yeast Rqc1 was reported to be a part of the RQC complex, no direct interaction between TCF25 and Listerin has been reported either. Interestingly, TCF25 was reported to interact with another E3 ligase, X-linked inhibitor of apoptosis (Steen and Lindholm, 2008). Given the few examples in which the basis for regulation of E2 activity and specificity by

other proteins has been determined, elucidation of TCF25's mechanism of action in executing this function will likely yield broadly applicable insights.

STAR METHODS

CONTACT FOR REAGENT AND RESOURCE SHARING

Further information and requests for resources and reagents should be directed to and will be fulfilled by the Lead Contact, Tatyana Pestova (tatyana.pestova@downstate.edu).

EXPERIMENTAL MODEL AND SUBJECT DETAILS

HEK293T cells were cultured in Dulbecco's Modified Eagle Medium (DMEM, Gibco), supplemented with 10% FBS (Gibco), 1X Glutamax (Gibco) and 1x penicillin/streptomycin (Gibco) at 37°C with 5% CO_2.

Recombinant proteins were expressed in *Escherichia coli* BL21(DE3) or Rosetta (DE3) cells grown in LB or 2×TY medium (1.6% tryptone, 1% yeast extract, 0.5% NaCl).

METHOD DETAILS

Construction of plasmids—Transcription vectors for MCHV, MVVHHC and MVVHHV mRNAs were made by GeneWiz (South Plainfield, NJ) analogously to the MVHC-STOP vectors (Pisareva et al., 2011).

Human Ptrh1 (*wt* and H46N and D121A mutants), PtrhD1 and $Ptrh2_{\Delta 1–62}$ lacking the N-terminal 62 amino acids (referred to here as Ptrh2) ORFs were inserted into pUC57 (GeneWiz) and then recloned between BamHI and SalI sites of pET28a for expression of C-terminally His_6-tagged proteins. pET28a-based vectors for bacterial expression of His_6-tagged human Npl4, and wt, $TAQ_{244–246}$→TAL and $TAQ_{244–246}$→GGQ mutant forms of ANKZF1 were prepared by GenScript (Piscataway, NJ). pcDNA3.1+/C-(K)DYK-based vectors for expression in human cells of C-terminally FLAG tagged human TCF25 and ANKZF1 were made using the CloneEZ strategy (GenScript).

β-VHP transcription vectors were designed essentially as described (Shao et al., 2013), with the exception of the introduction of 12 synonymous codon substitutions to eliminate rare codons and substitution of 4 non-conserved codons by AUG triplets to increase radiolabeling of β-VHP. β-VHP ORFs were preceded by an upstream T7 promoter and the native β-globin 5'UTR, and were cloned intopUC57 (GeneWiz). The initial vector encoded a 103aa polypeptide with a 3'-terminal Val (GUC) codon, followed by a SalI (+2nt after the last sense codon) restriction site or a stop codon followed by XbaI (+3nt after the last sense codon), BspHI (+9nt after the last sense codon), MscI (+13nt after the last sense codon), NcoI (+18nt after the last sense codon) and HindIII (+97nt after the last sense codon) restriction sites to create 3'UTRs of different lengths. This plasmid was restricted with FokI, PvuII, BamHI or EcoNI to produce non-stop mRNAs with ORFs of 66aa, 44aa, 35aa or 14aa respectively. β-VHP-Val with 3'-terminal Val (GUG) codon had a MscI (+1nt after the last sense codon) restriction site. β-VHP-Ser had an additional 3'-terminal Ser (UCU) codon and a XbaI (+2nt after the last sense codon) restriction site; β-VHP-Cys had an additional 3'-terminal Cys (UGC) codon and FspI (+0nt after the last sense codon) restriction site;

variants with partial β-VHP ORFs (45aa, 55aa, 75aa long, scheme in Figure 2E) all had a 3'-terminal Val (GUC) codon. Variants containing linkers (Figure 2C) were made by inserting cDNA corresponding to soluble/flexible linkers $[EGKSSGSGSESKST]_3$ or $[GGGGS]_9$ after the 49th or 102nd amino acid residue of the β-VHP ORF. Vectors for transcription of mRNAs encoding β-VHP with unstructured N-terminal extensions (Figure 5D) were made (GeneWiz) by inserting sequences encoding a.a. 34–68, a.a. 24–68 or a.a 15–68 of human Sec61β (Genbank: NP_006799.1) upstream of the β-VHP ORF.

mRNA and tRNA preparation—β-VHP plasmids were linearized at appropriate restriction sites prior to transcription. The GUS transcription vector was linearized using MscI to transcribe mRNA encoding a 207 aa-long GUS fragment (+1nt after the last sense codon). The β-globin plasmid was linearized with SalI to transcribe mRNA encoding 147 amino acids (+2nt after the last sense codon). $tRNA^{Ser}$-AGA, $tRNA^{Val}$-CAC and $tRNA_i^{Met}$ plasmids were linearized with BstNI. All mRNAs and tRNAs were transcribed using T7 RNA polymerase. Labeled $tRNA^{Ser}$ and $tRNA^{Val}$ were transcribed in the presence of $[\alpha^{32}P]$CTP (3000Ci(111 Tbq)/mmol).

Total (Σ) native tRNA was purified from 200 ml of the RRL post-ribosomal fraction (Pisarev et al., 2007). This fraction was dialyzed against buffer A (20 mM Tris-HCl, pH 7.5, 4 mM $MgCl_2$, 250 mM KCl, 2 mM DTT) and loaded on a DE52 column equilibrated with this buffer. The column was then washed with buffer A, and tRNA was eluted with buffer B (20 mM Tris-HCl, pH 7.5, 3 mM $MgCl_2$, 700 mM NaCl, 2 mM DTT). The tRNA was precipitated with ethanol, resuspended in 5ml of buffer C (100 mM Tris-HCl, pH 7.5, 5 mM $MgCl_2$), extracted with an equal volume of phenol-chloroform and precipitated with ethanol. The resulting tRNA was resuspended in buffer D (10 mM Tris-HCl, pH 7.5, 3 mM $MgCl_2$) and loaded on a G75 column equilibrated with buffer D + 100mM KCl. The peak fractions were precipitated, and tRNA was dissolved in buffer D at 400–500 A_{260} OD/ml.

Purification of factors and ribosomal subunits, and aminoacylation of tRNA—Native 40S and 60S subunits, eIF2, eIF3, eIF5B, eEF1H, eEF2, ABCE1 and total aminoacyl-tRNA synthetases were purified from RRL as described (Pisarev et al., 2007; Pisarev et al, 2010). Recombinant His_6-tagged eIFs 1, 1A, 4A, 4B, $4G_{736–1115}$, 5, eRF1, eRF1(AGQ), eRF3, Pelota and Hbs1 were expressed in *E. coli* and purified as described (Pisarev et al., 2007; Pisarev at al., 2010; Pisareva et al., 2011).

Native eIF5A was purified from RRL. A 40–50% ammonium sulfate (A.S.) precipitation fraction of a 0.5 M KCl ribosomal salt wash was prepared from 6 L of RRL as described (Pisarev et al., 2007). This fraction was dialyzed against buffer E (20 mM Tris-HCl, pH 7.5, 10% glycerol, 2 mM DTT, 0.1 mM EDTA) supplemented with 100 mM KCl and applied to a DE52 column equilibrated with buffer E + 100 mM KCl. The buffer E + 250 mM KCl elution fraction was dialyzed against buffer E + 100 mM KCl and applied to a P11 column equilibrated with buffer E + 100 mM KCl. The buffer E + 400 mM KCl elution fraction was further purified on an FPLC MonoQ 5/50 GL column across a 100–500 mM KCl gradient, with eIF5A eluting at ~250 mM KCl. This fraction was applied to a hydroxyapatite column. Fractions were collected across a 20–500 mM phosphate buffer (pH 7.5) gradient, and eIF5A was eluted at ~230 mM phosphate buffer.

Deacylated native ΣtRNA was prepared by incubating ΣtRNA in 500mM Tris-HCl, pH 9 for 30 min at 37°C. Aminoacylation of $tRNA^{Ser}$-AGA, $tRNA^{Val}$-CAC, $tRNA^{Met}$ and native ΣtRNA was done in the presence of serine, valine, methionine or all amino acids, respectively, using total native aminoacyl-tRNA synthetases as described (Pisarev et al., 2007).

Preparation of 80S RNCs, 60S RNCs and free peptidyl-tRNA—To prepare 60S/80S RNCs, 250 nM β-VHP, β-globin or GUS mRNAs were translated using the Flexi RRL system (Promega) in the presence of [^{35}S]-methionine (>1000Ci (37.0TBq)/mmol), or in the case of Figures 2B, 7A-C, 7E and S6D, in the presence of Ser-[^{32}P]$tRNA^{Ser}$ or Val-[^{32}P]$tRNA^{Val}$. When mRNAs containing a termination codon were used, reaction mixtures were also supplemented with 1.5 μM eRF1(AGQ) and 1.5 μM eRF3. Translation mixtures were incubated for 50 min at 32°C and subjected to centrifugation in a Beckman SW55 rotor at 53,000 rpm for 95 min at 4°C in 10%–30% linear sucrose density gradients prepared in buffer F (20 mM Tris pH 7.5, 100 mM KCl, 1.5 mM $MgCl_2$, 2 mM DTT and 0.25 mM spermidine), yielding 80S RNCs and small amounts of “native” 60S RNCs. To obtain 60S RNCs from 80S RNCs, the latter were incubated with ABCE1, Pelota and Hbs1 in the presence of vacant 60S subunits and subjected to the second round of SDG centrifugation (Pisareva et al., 2011). “Native” 60S RNCs were also purified further by the second round of centrifugation.

To prepare free peptidyl-tRNAs, 80S-RNCs were treated with 5mM EDTA and also subjected to 10%−30% SDG centrifugation. Free peptidyl-tRNA was found in the top fractions.

To reconstitute 80S RNCs with short peptides, 75 nM MCHV, MVHC, MVVHHC or MVVHHV mRNAs were incubated with 125 nM 40S ribosomal subunits, 500 nM eIF1, 500 nM eIF1A, 150 nM eIF2, 150 nM eIF3, 500 nM eIF4A, 250 nM eIF4B, 500 nM $\Delta 4G_{736–1115}$ and 250 nM Met-$tRNA^{Met}$ (or [^{35}S]Met-$tRNA^{Met}$ in the case of MVVHHV mRNA) in buffer G (20mM Tris-HCl pH7.5, 100mM KCl, 2.5mM $MgCl_2$, 0.25mM spermidine, 2mM DTT) supplemented with 0.2 mM GTP, 1mM ATP and 2 U/μl RiboLock RNase inhibitor for 10 min at 37°C. Assembled 48S initiation complexes were then incubated with 170 mM 60S subunits, 430 nM eIF5 and 65 nM eIF5B for 10 min at 37°C to obtain 80S initiation complexes. To form 80S RNCs, 80S initiation complexes were mixed with 20 nM eEF1H, 20 nM eEF2 and aminoacylated native ∑tRNA (aminoacylated with a mixture of unlabeled amino acids and [^{35}S]Cysteine (>1000Ci (37.0TBq)/mmol), except for MVVHHV mRNA, in which case all amino acids were unlabeled), and incubation continued for another 10 min. The resulting 80S RNCs were purified by 10%−30% SDG centrifugation as described above.

Purification of native Ptrh1 and Slfn14—Native Prth1 was purified from HeLa cells on the basis of its activity in releasing nascent polypeptides from 60S RNCs formed on non-stop β-VHP mRNA. HeLa cell extract was prepared from 300 ml of HeLa cell pellet. Cells were resuspended in two volumes of buffer H (10mM Tris-HCl pH7.5, 20mM KCl, 1.5mM $MgCl_2$, 2mM DTT, 0.1mM EDTA). After incubation for 30min, cells were lysed by Dounce homogenization, after which one third volume of buffer I (20mM Tris-HCl pH7.5, 50mM

KCl, 2mM $MgCl_2$, 1M sucrose) was added to the cell lysate. Cell debris was removed by centrifugation for 20 min at 15,000 rpm at 4°C and the supernatant was stored at −80°C. To prepare HeLa cell extract for the experiment shown in Figure 5F, a small portion of lysate was dialyzed against buffer J (20mM Tris-HCl, pH7.5, 100 mM KCl, 1.5mM $MgCl_2$, 10% glycerol, 2mM DTT, 0.1mM EDTA). For purification of Ptrh1, the rest of the extract was used for preparation of 0.5 M KCl ribosomal salt wash and subsequent fractionation by ammonium sulfate precipitation (Pisarev et al., 2007). Initially, the activity was found in the 0%–40% A.S. precipitation fraction of the 0.5 M KCl ribosomal salt wash obtained from 300 ml HeLa cells (Pisarev et al., 2007). This fraction was dialyzed against buffer E + 100 mM KCl and applied to a DE52 column equilibrated with buffer E + 100 mM KCl. The active flow-through fraction was applied to a P11 column equilibrated with buffer E + 100 mM KCl, and the activity was eluted with buffer E + 1000 mM KCl. After dialysis, this fraction was applied to an FPLC MonoS 5/50 GL column. Fractions were collected across a 100–500 mM KCl gradient. The activity was eluted at ~350 mM KCl and applied to a hydroxyapatite column. Fractions were collected across a 20–500 mM phosphate buffer (pH 7.5) gradient. The activity was eluted at 130–180 mM phosphate buffer, and was identified as Ptrh1 by comparing the protein composition of fractions with and without nascent polypeptide releasing activity by LC-MS/MS (Rockefeller University Proteomics Resource Center, New York, NY) [Supplemental Table 1].

Native Slfn14 was purified from RRL on the basis of its activity in releasing nascent polypeptides linked to truncated tRNA from 60S RNCs formed on non-stop β-VHP mRNA. Initially, the activity was found in the 0%–40% A.S. precipitation fraction of the 0.5 M KCl ribosomal salt wash obtained from 3 L of RRL (Pisarev et al., 2007). This fraction was dialyzed against buffer E + 100 mM KCl and loaded on a DE52 column equilibrated with buffer E + 100 mM KCl. The flow-through fraction was applied to a P11 column equilibrated with buffer E + 100mM KCl, and the activity was eluted by buffer E + 400 mM KCl. After dialysis, this fraction was applied to an FPLC MonoQ 5/50 GL column. Fractions were collected across a 100–500 mM KCl gradient, and the activity was eluted in the flow-through. The flow-through was loaded on a hydroxyapatite column, and fractions were collected across a 20–500 mM phosphate buffer (pH 7.5) gradient. The activity was eluted at ~350mM phosphate buffer. This fraction was applied to a MonoS 5/50 GL column. Fractions were collected across a 100–500 mM KCl gradient, and the activity was eluted at ~420 mM KCl. It was identified as Slfn14 by LC-MS/MS analysis of the purified single protein band (Rockefeller University Proteomics Resource Center) [Supplemental Table 2].

Purification of recombinant Ptrh1, Ptrh2, PtrhD1, ICT1 and Pth—Ptrh1 (*wt* and H46N and D121A mutants), Ptrh2, PtrhD1 and ICT1 were expressed in 2 L *E. coli* BL21(DE3). Protein expression was induced with 0.1 mM IPTG for Ptrh1, PtrhD1 and ICT1 and 1 mM IPTG for Ptrh2, and cells were grown for 3 h at 37°C for Ptrh2 and for 16 h at 16°C for Ptrh1, PtrhD1 and ICT1. All proteins were purified by Ni-NTA chromatography followed by FPLC on a MonoS 5/50 GL. Pth was expressed by growing *E. coli* BL21(DE3) at 37°C in 2 L of 2xTY medium until the stationary phase of growth, inducing Pth expression with 1 mM IPTG and continuing incubation for 4 h at 18°C. Pth was purified by Ni-NTA chromatography followed by FPLC on a MonoS 5/50 GL column.

Purification of Listerin, NEMF, TCF25, ANKZF1, p97, Ufd1 and Npl4—For purification of Listerin, NEMF, TCF25 and ANKZF1 from mammalian cells, they were transiently expressed in HEK293T cells and isolated by FLAG affinity chromatography as described (Shao and Hegde, 2014; Shao et al., 2015). For purification of *wt*, $TAQ_{244–246}$→TAL and $TAQ_{244–246}$→GGQ mutant forms of ANKZF1 from bacterial cells, they were expressed in 4 L of *E. coli* BL21 (DE3). Protein expression was induced with 0.5 mM IPTG for 16h at 16°C. All proteins were purified by Ni-NTA chromatography.

p97 (wt and K251A and R638A mutants) was expressed in 2 L of E. coli BL21(DE3). Protein production was induced with 1 mM IPTG for 3 h at 37°C. Proteins were purified by Ni-NTA chromatography followed by FPLC on a MonoQ 5/50 GL column. To confirm the enzymatic activity of purified p97 (Figure S4B), 100 nM wt or mutant p97 were incubated with 20 nM [γ–^{32}P]ATP 6000Ci/mmol) and 30 μM cold ATP for 5 min at 37°C in buffer K (20 mM Tris pH 7.5, 100 mM KCl, 8 mM MgCl, 2 mM DTT, 0.25 mM spermidine). [γ–^{32}P]ATP and [^{32}P]P_i were resolved by TLC on polyethyleneimine cellulose by spotting 1.5 μL aliquots onto the plates for chromatography done using 0.8 M LiCl/0.8 M acetic acid, followed by autoradiography.

Ufd1 and Npl4 were expressed in 4 L of *E. coli* Rosetta (DE3). Protein expression was induced with 0.5 mM IPTG for 4 h at 37°C. Ufd1 and Npl4 were purified by affinity chromatography on Ni-NTA agarose. Ufd1 was purified further by FPLC on a MonoQ 5/50 GL column, collecting fractions across a 100–500 mM KCl gradient. To form the Ufd1-Npl4 heterodimer, purified Ufd1 and Npl4 were incubated for 10 min at 37°C. The Ufd1-Npl4 heterodimer was separated by FPLC on a MonoQ 5/50 GL column using a 100–500 mM KCl gradient.

In vitro translation (Figures 1B, 2I and S1F-G)—250 nM β-VHP mRNAs containing the indicated number of nucleotides after the last sense codon were translated in RRL at 32°C in the absence (Figure 1B) or in the presence of 120 nM Ptrh1 (Figure S1F) or 240 nM Slfn14 (Figure S1G). When indicated, after translation, reaction mixtures were treated with 60 μg/ml RNaseA for 10 minutes at 32°C. In Figure 2I, following translation of β-VHP mRNA in RRL for 50 minutes at 32°C, reaction mixtures were incubated with 360 nM Ptrh1 or 2 mM puromycin. Reactions were stopped at the indicated times by addition of loading buffer and heating for 2 minutes at 90°C. In all cases, proteins were resolved by 4–12% SDS-PAGE and visualized by autoradiography.

Release of non-ubiquitinated nascent chains from 60S and 80S RNCs by Ptrh1, Ptrh2, EcPth, PtrhD1, ICT1, Slfn14 and puromycin (Figures 1, 2, 4A, S1-S3, S5A and S5D)—Unless otherwise indicated, the reactions were done in buffer G (containing 2.5 mM $MgCl_2$ or the indicated $MgCl_2$ concentration, and supplemented with 1 mM ATP, 0.4 mM GTP and 2 U/μl RiboLock RNase inhibitor) using the indicated combinations of the following components: 5 nM [^{35}S]Met-labeled 80S-RNCs, 60S-RNCs or free βVHP-tRNA, 5 nM [^{32}P]$tRNA^{Ser}$-containing 80S RNCs, 5 nM free [^{35}S]Cys-MCHV-tRNA, 1–3 μL of protein fractions tested during isolation of native Ptrh1 and Slfn14, 7.5 nM *wt* or mutant Ptrh1, 7.5 nM Ptrh2, 7.5 nM Pth, 7.5 nM PtrhD1, 7.5 nM ICT1, 25 nM Slfn14, 2 mM puromycin, 50 nM eRF1/eRF3, 200 nM Pelota, 30 nM ABCE1, 50 nM Hbs1,

1.4 μM deacylated $tRNA^{Ser}$, 100 nM eRF1(AGQ)/eRF3 and 0.4 mM GMPPNP, 100 nM eIF5A, 2 mM cycloheximide, 60 nM Listerin and 60 nM NEMF, and incubated at 37°C for 5 min or as indicated. 20 μL samples were resolved by 4−12% SDS−PAGE and proteins were visualized by autoradiography. Where indicated, protein bands were quantified using a Typhoon Phosphorimager and ImageQuant software. In some experiments, 100 μL aliquots of the reaction mixtures were analyzed by 10%−30% SDG centrifugation at 53,000 rpm for 95 min at 4°C, and labeled nascent peptides were quantified by liquid scintillation counting.

Ubiquitination and deubiquitination (Figures 3, S4, 6G and S5E)—Ubiquitination of nascent chain peptides was performed essentially as described (Shao et al., 2013). Unless otherwise indicated, 5 nM SDG-purified [^{35}S]Met-labeled 60S RNCs were incubated with the indicated combinations of 80 nM Ube1, 250 nM Ube2D family proteins (Ube2D1–4), 250 nM other Ube2 family proteins (Ube2A, Ube2B, Ube2C, Ube2E1, Ube2E3, Ube2F, Ube2G1, Ube2H, Ube2J1, Ube2J2, Ube2K, Ube2L3, Ube2N/V1, Ube2N/V2, Ube2Q1–2, Ube2Q2–1, Ube2R1, Ube2R2, Ube2S, Ube2T, Ube2W2 and Ube2Z), 60 nM Listerin, 60 nM NEMF, 7.5 μM ubiquitin (*wt*, K48R, K29/48/63R, K6-only, K11-only, K27-only, K29-only, K33-only, K48-only or K63-only), 150 nM p97, 150 nM Ufd1/Npl4 complex, 60 nM TCF25, 200 nM ANKZF1 and 7.5 μM S5a in buffer G supplemented with 1 mM ATP, 0.4 mM GTP, 12 mM creatine phosphate, 20 μg/ml creatine kinase, and 2 U/μl RiboLock RNase inhibitor for 10 min at 37°C. In all experiments, 20 μL samples were resolved by 4−12% SDS−PAGE, and proteins were visualized by autoradiography.

Ubiquitination of S5a and p53 substrates by MDM2 ubiquitin ligase was done using the respective ubiquitin ligase kits (Boston Biochem). Reactions were prepared according to the manufacturer's recommended protocol and supplemented with 1 mM ATP, 60 nM TCF25, and 10 μM ubiquitin (*wt*, K48R, K11-only, K33-only, K48-only or K63-only). Ubiquitination was visualized by western blotting using anti-S5a and anti-p53 antibodies.

In deubiquitination experiments (Figure 3L), [^{35}S]Met-labeled 60S-RNCs were ubiquitinated with or without TCF25, purified by SDG centrifugation and incubated with 1.5 μM Otub1, Yod1, or Usp2 for 30 min at 37°C, after which 20 μL samples were resolved by 4−12% SDS−PAGE, and proteins were visualized by autoradiography.

Release of ubiquitinated nascent chains from 60S RNCs by Ptrh1 and puromycin (Figures 4B-F and S5B-C)—Release of ubiquitinated nascent chains from 60S RNCs was assayed either directly in ubiquitination reactions or using SDG purified ubiquitinated 60S RNCs as a substrate. In the first case, ubiquitination of [^{35}S]Met-labeled 60S RNCs was performed for the indicated times in the presence or absence of NEMF essentially as described above, after which reaction mixtures were supplemented with 20 nM Ptrh1 or 2 mM puromycin, and incubation continued for an additional 5–10 minutes (except for experiments in S5C, in which puromycin was added simultaneously with ubiquitinating enzymes in the presence or absence of TCF25). In the second case, SDG-purified [^{35}S]Met-labeled 60S RNCs were incubated in buffer G (supplemented with 1 mM ATP, 0.4 mM GTP and 2 U/μl RiboLock RNase) for 10 minutes at 37°C with 2 mM puromycin directly or with 20 nM Ptrh1 after deubiquitination by Otub1, Yod1 or Usp2. Samples were then resolved by 4−12% SDS−PAGE followed by visualization of protein bands by autoradiography, or

analyzed by 10%−30% SDG centrifugation at 53,000 rpm for 95 min at 4°C followed by quantitation of labeled nascent peptides by liquid scintillation and subsequent analysis of fractions corresponding to RNCs and free NC/NC-tRNAs by 4−12% SDS−PAGE.

Proteasomal degradation (Figures 5, 6C and S5E-G)—Human 26S proteasome was purchased from Boston Biochem. Proteasomal degradation of ubiquitinated nascent chains was assayed in buffer G (supplemented with 1 mM ATP, 0.4 mM GTP, 12 mM creatine phosphate, 20 μg/ml creatine kinase, and 2 U/μl RiboLock RNase inhibitor) either directly in ubiquitination mixtures (in the presence or absence of NEMF or TCF25) or using SDG purified ubiquitinated 60S RNCs as a substrate, followed by addition of the indicated combinations of 30 nM 26S proteasome, 2 mM puromycin, 240nM ANKZF1, 20 nM Ptrh1, HeLa cell extract, 150 nM p97, 150 nM Ufd1/Npl4 complex, 1.0 μM Yod1, 60 nM Listerin, 60 nM NEMF, 100 nM eRF1, 100 nM eRF3, 30 nM ABCE1, 20 nM ICT1 and 4.5 μM native deacylated ∑tRNAs, and incubation for 30–45 min at 37°C, or as indicated. Samples were resolved by 4−12% SDS−PAGE. Proteins were visualized by autoradiography, and in Figure 6C also quantitated using a Typhoon Phosphorimager and ImageQuant software.

ANKZF1-mediated cleavage of tRNA in 60S RNCs (Figures 6B, 6D-F, 7A-D, S6)—Cleavage reactions were done in buffer G (supplemented with 1 mM ATP, 0.4 mM GTP, 12 mM creatine phosphate, 20 μg/ml creatine kinase, and 2 U/μl RiboLock RNase inhibitor) with the indicated combinations of the following components: 5 nM [^{35}S]Met-labeled non-ubiquitinated 60S-RNCs, 80S RNCs, SDG-purified ubiquitinated 60S-RNCs or free β-VHP-tRNA, 5 nM [^{32}P]tRNA^{Val}- or [^{32}P]tRNA^{Ser}- containing 60S RNCs, 100nM β-VHP mRNA or [^{32}P]tRNA^{Val}, 240nM *wt* or mutant ANKZF1, 60nM Listerin, 60nM NEMF, 150 nM p97, 150 nM Ufd1/Npl4 complex, 80 nM Ube1, 250 nM Ube2D1 and 7.5 μM *wt* ubiquitin. Reaction mixtures were incubated at 37°C for 45 min or as indicated. In Figures 6D-F, 7A-B, 7D and S6A-B, samples were resolved by 4−12% SDS−PAGE followed by autoradiography. In Figure 6E, protein bands were quantified using a Typhoon Phosphorimager and ImageQuant software. In Figure 6B, reactions were analyzed by 10% −30% SDG centrifugation at 53,000 rpm for 95 min at 4°C, and labeled nascent peptides were detected by liquid scintillation and then resolved by 4−12% SDS−PAGE followed by autoradiography. In Figures 7C and S6C-D, samples were phenol-extracted and analyzed using 6% sequencing gel.

Analysis of ribosomal binding of ANKZF1, NEMF, Ptrh1, Ptrh2 and EcPth (Figures 6H and S3H)—300 nM NEMF, ANKZF1, Ptrh1, Ptrh2 or Pth, were incubated with 300 nM 40S subunits, 60S subunits or 80S ribosomes in buffer G supplemented with 1 mM ATP, 0.4 mM GTP and 2 U/μl RiboLock RNase inhibitor for 10 min at 37°C. The reaction mixtures were then subjected to 10%−30% SDG centrifugation at 53,000 rpm for 95 min at 4°C. Gradient peak fractions corresponding to 80S ribosomes and ribosomal subunits were analyzed by 4−12% SDS−PAGE followed by SYPRO Staining (Invitrogen) and blotting with anti-ANKZF1, anti-FLAG, anti-Ptrh1, anti-Ptrh2 or anti-His_6 tag antibodies, as indicated.

Electrophoretic mobility shift assay (Figure 6I)—300 nM ANKZF1 or NEMF were incubated with 100 nM [^{32}P]tRNA^{Val} or [^{32}P]tRNA^{Ser} in 20 μl reaction mixtures containing buffer G supplemented with 1 mM ATP, 0.4 mM GTP and 2 U/μl RiboLock RNase inhibitor for 10 min at 37°C. After addition of 2 μl loading buffer (15% glycerol and 0.1% bromophenol blue), samples were applied to non-denaturing 6% acrylamide gels (with the acrylamide/bis-acrylamide ratio of 75:1) and subjected to electrophoresis at 4°C. Labeled tRNA and tRNA-protein complexes were detected by autoradiography.

The influence of aminoacylated and deacylated ΣtRNA on 60S RNCs (Figures 7E-G)—5 nM [^{35}S]Met-labeled or [^{32}P]tRNA^{Val}-containing 60S RNCs were incubated for 30 minutes at 37°C in buffer G (supplemented with 1 mM ATP, 0.4 mM GTP and 2 U/μl RiboLock RNase inhibitor) with indicated combinations of 4.5 μM deacylated native ∑tRNAs, 2 μM aminoacylated native ∑tRNAs, 60 nM Listerin, 60 nM NEMF and 100 nM eEF2. Samples were resolved by 4−12% SDS−PAGE followed by autoradiography.

Multiple sequence alignment (Figure S1C)—Full-length amino acid sequences were aligned using Clustal Omega (https://www.ebi.ac.uk/Tools/msa/clustalo/) and visualized with JalView.

Multiple sequence alignment (Figure S7)—Full-length amino acid sequences were aligned using Clustal Omega (https://www.ebi.ac.uk/Tools/msa/clustalo/) and amino acid sequences of individual domains were then aligned using T-Coffee (https://www.ebi.ac.uk/Tools/msa/tcoffee/), in both instances using default parameters. Alignments were rendered visually using ESPript 3 (http://espript.ibcp.fr).

Prediction of secondary structure (Figure S7)—Secondary structure elements were predicted using Phyre2 (www.sbg.bio.ic.ac.uk/~phyre2/) and I-TASSER (https://zhanglab.ccmb.med.umich.edu/I-TASSER/).

Supplementary Material

Refer to Web version on PubMed Central for supplementary material.

ACKNOWLEDGMENTS

We thank Nono Takeuchi and Kosuke Ito for vectors for expression of ICT1 and *E. coli* Pth, respectively, Manu Hegde and Susan Shao for pcDNA-based vectors for expression of NEMF and Listerin, protocols for purification of these proteins and helpful advice, Alexei Kisselev for helpful discussion and Andrew Tcherepanov for expert technical assistance. This work was supported by NIH grants GM122602 and GM80623 to T.V.P, and NIH grant AI123406 to C.U.T.H. K.K. was supported in part by the Uehara Memorial Foundation.

REFERENCES

Akabane S, Ueda T, Nierhaus KH, and Takeuchi N (2014). Ribosome rescue and translation termination at non-standard stop codons by ICT1 in mammalian mitochondria. PLoS Genet 10, e1004616. [PubMed: 25233460]

Balchin D, Hayer-Hartl M, and Hartl FU (2016). In vivo aspects of protein folding and quality control. Science 353, aac4354.

Bodnar NO, and Rapoport TA (2017). Molecular mechanism of substrate processing by the Cdc48 ATPase complex. Cell 169, 722–735. [PubMed: 28475898]

Brandman O, Stewart-Ornstein J, Wong D, Larson A, Williams CC, Li GW, Zhou S, King D, Shen PS, Weibezahn J et al. (2012). A ribosome-bound quality control complex triggers degradation of nascent peptides and signals translation stress. Cell 151, 1042–1054. [PubMed: 23178123]

Brandman O, and Hegde RS (2016). Ribosome-associated protein quality control. Nat. Struct. Mol. Biol 23, 7–15 [PubMed: 26733220]

Burks GL, McFeeters H, and McFeeters RL (2016). Expression, purification, and buffer solubility optimization of the putative human peptidyl-tRNA hydrolase PTRHD1. Protein Expr Purif 126, 49–54. [PubMed: 27235175]

DeLaBarre B, Christianson JC, Kopito RR, and Brunger AT (2006). Central pore residues mediate the p97/VCP activity required for ERAD. Mol. Cell 22, 451–462. [PubMed: 16713576]

de Pereda JM, Waas WF, Jan Y, Ruoslahti E, Schimmel P, and Pascual J (2004). Crystal structure of a human peptidyl-tRNA hydrolase reveals a new fold and suggests basis for a bifunctional activity. J. Biol. Chem 279, 8111–8115. [PubMed: 14660562]

Defenouillère Q, Yao Y, Mouaikel J, Namane A, Galopier A, Decourty L, Doyen A, Malabat C, Saveanu C, Jacquier A et al. (2013). Cdc48-associated complex bound to 60S particles is required for the clearance of aberrant translation products. Proc. Natl. Acad. Sci. U.S.A 110, 5046–5051. [PubMed: 23479637]

Eddins MJ, Carlile CM, Gomez KM, Pickart CM, and Wolberger C (2006). Mms2-Ubc13 covalently bound to ubiquitin reveals the structural basis of linkage-specific polyubiquitin chain formation. Nat. Struct. Mol. Biol 13, 915–920. [PubMed: 16980971]

Edelmann MJ, Iphöfer A, Akutsu M, Altun M, di Gleria K, Kramer HB, Fiebiger E, Dhe-Paganon S, and Kessler BM (2009). Structural basis and specificity of human otubain 1-mediated deubiquitination. Biochem J 418, 379–390. [PubMed: 18954305]

Hentzen D, Mandel P, and Garel JP (1972). Relation between aminoacyl-tRNA stability and the fixed amino acid. Biochim. Biophys. Acta 281, 228–232. [PubMed: 4629424]

Heo JM, Livnat-Levanon N, Taylor EB, Jones KT, Dephoure N, Ring J, Xie J, Brodsky JL, Madeo F, Gygi SP et al. (2010). A stress-responsive system for mitochondrial protein degradation. Mol. Cell 40, 465–480. [PubMed: 21070972]

Heo JM, Nielson JR, Dephoure N, Gygi SP, and Rutter J (2013). Intramolecular interactions control Vms1 translocation to damaged mitochondria. Mol. Biol. Cell 24, 1263–1273. [PubMed: 23468520]

Huter P, Müller C, Arenz S, Beckert B, and Wilson DN (2017). Structural basis for ribosome rescue in bacteria. Trends Biochem. Sci 42, 669–680. [PubMed: 28629612]

Inada T (2017). The ribosome as a platform for mRNA and nascent polypeptide quality control. Trends Biochem. Sci 42, 5–15. [PubMed: 27746049]

Ito K, Qi H, Shimizu Y, Murakami R, Miura K, Ueda T, and Uchiumi T (2011). Crystallization and preliminary X-ray analysis of peptidyl-tRNA hydrolase from *Escherichia coli* in complex with the acceptor-TΨC domain of tRNA. Acta. Crystallogr. Sect. F. Struct. Biol. Cryst. Commun 67, 1566–1569.

Ivanova EV, Kolosov PM, Birdsall B, Kelly G, Pastore A, Kisselev LL, and Polshakov VI (2007). Eukaryotic class 1 translation termination factor eRF1--the NMR structure and dynamics of the middle domain involved in triggering ribosome-dependent peptidyl-tRNA hydrolysis. FEBS J 274, 4223–4237. [PubMed: 17651434]

Izawa T, Park SH, Zhao L, Hartl FU, and Neupert W (2017). Cytosolic protein Vms1 links ribosome quality control to mitochondrial and cellular homeostasis. Cell 171, 890–903. [PubMed: 29107329]

Jin H, Kelley AC, Loakes D, and Ramakrishnan V (2010). Structure of the 70S ribosome bound to release factor 2 and a substrate analog provides insights into catalysis of peptide release. Proc. Natl. Acad. Sci. USA 107, 8593–8598. [PubMed: 20421507]

Kim HT, Kim KP, Uchiki T, Gygi SP, and Goldberg AL (2009). S5a promotes protein degradation by blocking synthesis of nondegradable forked ubiquitin chains. EMBO J 28, 1867–1877. [PubMed: 19387488]

Kostova KK, Hickey KL, Osuna BA, Hussmann JA, Frost A, Weinberg DE, and Weissman JS (2017). CAT-tailing as a fail-safe mechanism for efficient degradation of stalled nascent polypeptides. Science 357, 414–417. [PubMed: 28751611]

Lyumkis D, Oliveira dos Passos D, Tahara EB, Webb K, Bennett EJ, Vinterbo S, Potter CS, Carragher B, and Joazeiro CA (2014). Structural basis for translational surveillance by the large ribosomal subunit-associated protein quality control complex. Proc. Natl. Acad. Sci. U.S.A 111, 15981–15986. [PubMed: 25349383]

Majorek KA, Dunin-Horkawicz S, Steczkiewicz K, Muszewska A, Nowotny M, Ginalski K, and Bujnicki JM (2014). The RNase H-like superfamily: new members, comparative structural analysis and evolutionary classification. Nucleic Acids Res 42, 4160–4179. [PubMed: 24464998]

McKnight CJ, Doering DS, Matsudaira PT, and Kim PS (1996). A thermostable 35-residue subdomain within villin headpiece. J. Mol. Biol 260, 126–134. [PubMed: 8764395]

Mevissen TE, Hospenthal MK, Geurink PP, Elliott PR, Akutsu M, Arnaudo N, Ekkebus R, Kulathu Y, Wauer T, El Oualid F et al. (2013). OTU deubiquitinases reveal mechanisms of linkage specificity and enable ubiquitin chain restriction analysis. Cell 154, 169–184. [PubMed: 23827681]

Middleton AJ, and Day CL (2015). The molecular basis of lysine 48 ubiquitin chain synthesis by Ube2K. Sci. Rep 5, 16793. [PubMed: 26592444]

Middleton AJ, Wright JD, and Day CL (2017). Regulation of E2s: A role for additional ubiquitin binding sites? J. Mol. Biol 429, 3430–3440. [PubMed: 28625848]

Miyoshi K, Tsukumo H, Nagami T, Siomi H, and Siomi MC (2005). Slicer function of Drosophila Argonautes and its involvement in RISC formation. Genes Dev 19, 2837–2848. [PubMed: 16287716]

Morse RP, Nikolakakis KC, Willett JL, Gerrick E, Low DA, Hayes CS, and Goulding CW (2012). Structural basis of toxicity and immunity in contact-dependent growth inhibition (CDI) systems. Proc. Natl. Acad. Sci. USA 109, 21480–21485. [PubMed: 23236156]

Nielson JR, Fredrickson EK, Waller TC, Rendón OZ, Schubert HL, Lin Z, Hill CP, and Rutter J (2017). Sterol oxidation mediates stress-responsive Vms1 translocation to mitochondria. Mol. Cell 68, 673–685. [PubMed: 29149595]

Ohtani N, Yanagawa H, Tomita M, and Itaya M (2004). Cleavage of double-stranded RNA by RNase HI from a thermoacidophilic archaeon, *Sulfolobus tokodaii* 7. Nucleic Acids Res 32, 5809–5819. [PubMed: 15520465]

Osuna BA, Howard CJ, Kc S, Frost A, and Weinberg DE (2017). In vitro analysis of RQC activities provides insights into the mechanism and function of CAT tailing. Elife 6, e27949. [PubMed: 28718767]

Pestova TV, and Kolupaeva VG (2002). The roles of individual eukaryotic translation initiation factors in ribosomal scanning and initiation codon selection. Genes Dev 16, 2906–2922. [PubMed: 12435632]

Pisarev AV, Skabkin MA, Pisareva VP, Skabkina OV, Rakotondrafara AM, Hentze MW, Hellen CU, and Pestova TV (2010). The role of ABCE1 in eukaryotic posttermination ribosomal recycling. Mol. Cell 37, 196–210. [PubMed: 20122402]

Pisarev AV, Unbehaun A, Hellen CU, and Pestova TV (2007). Assembly and analysis of eukaryotic translation initiation complexes. Methods Enzymol 430, 147–177. [PubMed: 17913638]

Pisareva VP, Skabkin MA, Hellen CU, Pestova TV, and Pisarev AV (2011). Dissociation by Pelota, Hbs1 and ABCE1 of mammalian vacant 80S ribosomes and stalled elongation complexes. EMBO J 30, 1804–1817. [PubMed: 21448132]

Pisareva VP, Muslimov IA, Tcherepanov A, and Pisarev AV (2015). Characterization of novel ribosome-associated endoribonuclease SLFN14 from rabbit reticulocytes. Biochemistry 54, 3286–3301. [PubMed: 25996083]

Schmitt E, Mechulam Y, Fromant M, Plateau P, and Blanquet S (1997). Crystal structure at 1.2 A resolution and active site mapping of Escherichia coli peptidyl-tRNA hydrolase. EMBO J 16, 4760–4769. [PubMed: 9303320]

Shao S, Brown A, Santhanam B, and Hegde RS (2015). Structure and assembly pathway of the ribosome quality control complex. Mol. Cell 57, 433–444. [PubMed: 25578875]

Shao S, and Hegde RS (2014). Reconstitution of a minimal ribosome-associated ubiquitination pathway with purified factors. Mol. Cell 55, 880–890. [PubMed: 25132172]

Shao S, von der Malsburg K, and Hegde RS (2013). Listerin-dependent nascent protein ubiquitination relies on ribosome subunit dissociation. Mol. Cell 50, 637–648. [PubMed: 23685075]

Shaw JJ, and Green R (2007). Two distinct components of release factor function uncovered by nucleophile partitioning analysis. Mol. Cell 28, 458–467. [PubMed: 17996709]

Shen PS, Park J, Qin Y, Li X, Parsawar K, Larson MH, Cox J, Cheng Y, Lambowitz AM, and Weissman JS et al. (2015). Rqc2p and 60S ribosomal subunits mediate mRNA-independent elongation of nascent chains. Science 347, 75–78. [PubMed: 25554787]

Song H, Mugnier P, Das AK, Webb HM, Evans DR, Tuite MF, Hemmings BA, and Barford D (2000). The crystal structure of human eukaryotic release factor eRF1--mechanism of stop codon recognition and peptidyl-tRNA hydrolysis. Cell 100, 311–321. [PubMed: 10676813]

Steen H, and Lindholm D (2008). Nuclear localized protein-1 (Nulp1) increases cell death of human osteosarcoma cells and binds the X-linked inhibitor of apoptosis protein. Biochem. Biophys. Res. Commun 366, 432–437. [PubMed: 18068114]

Stewart MD, Ritterhoff T, Klevit RE, and Brzovic PS (2016). E2 enzymes: more than just middle men. Cell Res 26, 423–440. [PubMed: 27002219]

Verma R, Oania RS, Kolawa NJ, and Deshaies RJ (2013). Cdc48/p97 promotes degradation of aberrant nascent polypeptides bound to the ribosome. Elife 2, e00308. [PubMed: 23358411]

Verma R, Reichermeier KM, Burroughs AM, Oania RS, Reitsma JM, Aravind L, and Deshaies RJ (2018). Vms1 and ANKZF1 peptidyl-tRNA hydrolases release nascent chains from stalled ribosomes. Nature 557, 446–451. [PubMed: 29632312]

Vivanco-Domínguez S, Bueno-Martínez J, León-Avila G, Iwakura N, Kaji A, Kaji H, and Guarneros G (2012). Protein synthesis factors (RF1, RF2, RF3, RRF, and tmRNA) and peptidyl-tRNA hydrolase rescue stalled ribosomes at sense codons. J. Mol. Biol 417, 425–439. [PubMed: 22326347]

Yau RG, Doerner K, Castellanos ER, Haakonsen DL, Werner A, Wang N, Yang XW, Martinez-Martin N, Matsumoto ML, Dixit VM, and Rape M (2017). Assembly and function of heterotypic ubiquitin chains in cell-cycle and protein quality control. Cell 171, 918–933. [PubMed: 29033132]

Ye Y, Akutsu M, Reyes-Turcu F, Enchev RI, Wilkinson KD, and Komander D (2011). Polyubiquitin binding and cross-reactivity in the USP domain deubiquitinase USP21. EMBO Rep 12, 350–357. [PubMed: 21399617]

Yu H, Kago G, Yellman CM, and Matouschek A (2016). Ubiquitin-like domains can target to the proteasome but proteolysis requires a disordered region. EMBO J 35, 1522–1536. [PubMed: 27234297]

Zinoviev A, Hellen CU, and Pestova TV (2015). Multiple mechanisms of reinitiation on bicistronic calicivirus mRNAs. Mol. Cell 57, 1059–1073. [PubMed: 25794616]

Zurita Rendón O, Fredrickson EK, Howard CJ, Van Vranken J, Fogarty S, Tolley ND, Kalia R, Osuna BA, Shen PS, Hill CP et al. (2018). Vms1p is a release factor for the ribosome-associated quality control complex. Nat. Commun 9, 2197. [PubMed: 29875445]

Highlights

- NC-tRNAs are not stably fixed in the P site of 60S RNCs and can be cleaved by Ptrh1
- Association with NEMF and ubiquitination of NCs accommodates NC-tRNAs in the P-site
- Accommodation of Ub-NC-tRNAs makes 60S RNCs Ptrh1-resistant but susceptible to ANKZF1
- ANKZF1 induces a specific cut in tRNA, releasing Ub-NCs linked to 4 tRNA nucleotides

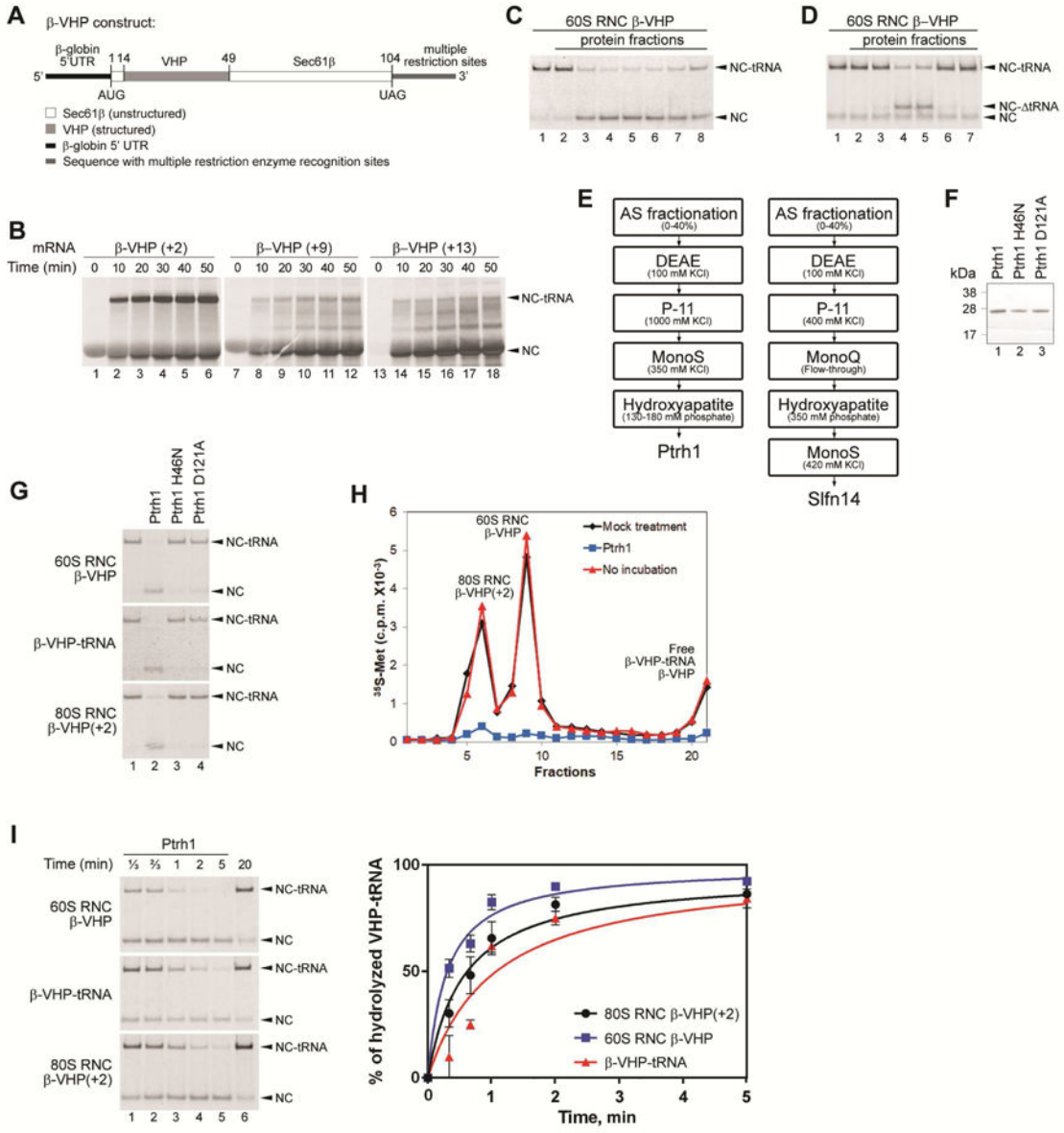

Figure 1. Release of non-ubiquitinated NCs from 60S and 80S RNCs by Ptrh1

(A) Structural diagram of the β-VHP construct. (B) Translation in RRL of β-VHP mRNAs containing indicated numbers of nts after the last sense codon. (C, D) Representative gels showing purification on (C) MonoS and (D) MonoQ of two activities responsible for β-VHP release from 60S RNCs, which were later identified and Ptrh1 and Slfn14, respectively. (E) Schemes for purification of Ptrh1 and Slfn14. (F) Purified recombinant *wt* and mutant Ptrh1. (G) Activity of *wt* and mutant Ptrh1 on free β-VHP-tRNA and on 60S and 80S RNCs formed on non-stop β-VHP mRNA. (H) Activity of *wt* Ptrh1 on 60S/80S RNCs formed on non-stop β-VHP mRNA, assayed by SDG centrifugation. The upper fractions were omitted for clarity. (I) Time courses of Ptrh1-mediated hydrolysis of 60S/80S RNC-bound and free β-VHP-tRNA (left panel). The efficiency of hydrolysis was quantified by Phosphorimager

(right panel). (B-D, F, G, I) Factors were resolved and NC release was assayed by SDS-PAGE.

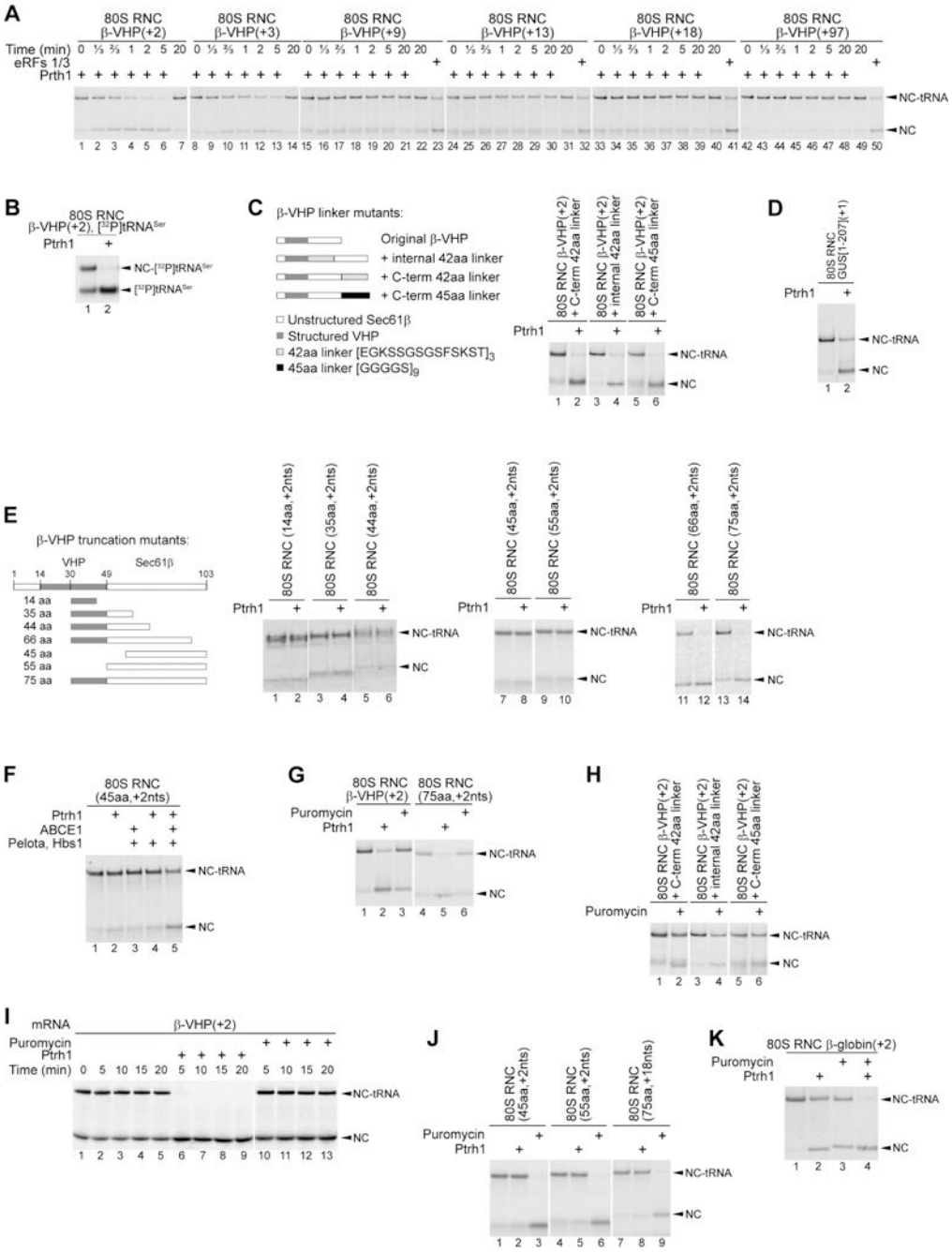

Figure 2. The activity of Ptrh1 on distinct types of 80S RNCs

(A) Time courses of Ptrh1-mediated hydrolysis of β-VHP-tRNA in 80S RNCs containing different numbers of mRNA nts after the P site. (B) Activity of Ptrh1 on 80S RNCs formed on mutant non-stop β-VHP mRNA with Ser as the last codon and containing [^{32}P]tRNA^{Ser}. (C) Schematic representation of β- VHP mutants containing linker insertions (left panel), and the activity of Ptrh1 on 80S RNCs formed on corresponding mutant non-stop mRNAs (right panel). (D) Activity of Ptrh1 on 80S RNCs assembled on non-stop mRNA encoding a.a. 1–207 of the GUS gene. (E) Schematic representation of β-VHP truncation mutants (left

panel), and the activity of Ptrh1 on 80S RNCs formed on corresponding mutant non-stop mRNAs (three right panels). (F) Activity of Ptrh1 on 80S RNCs formed on non-stop truncation mutant mRNA (shown in Figure 2E, left panel) in the presence of ABCE1/Pelota/Hbs1. (G, H, J, K) Comparison of the activities of Ptrh1 and puromycin on 80S RNCs formed on *wt* and mutant (shown in Figures 2C and2E, left panel) β-VHP mRNAs (G, H, J), and non-stop mRNA encoding β-globin (K). (I) Addition of Ptrh1 and puromycin to RRL following translation of non-stop β-VHP mRNA. (A-K) All activities were assayed by SDS-PAGE.

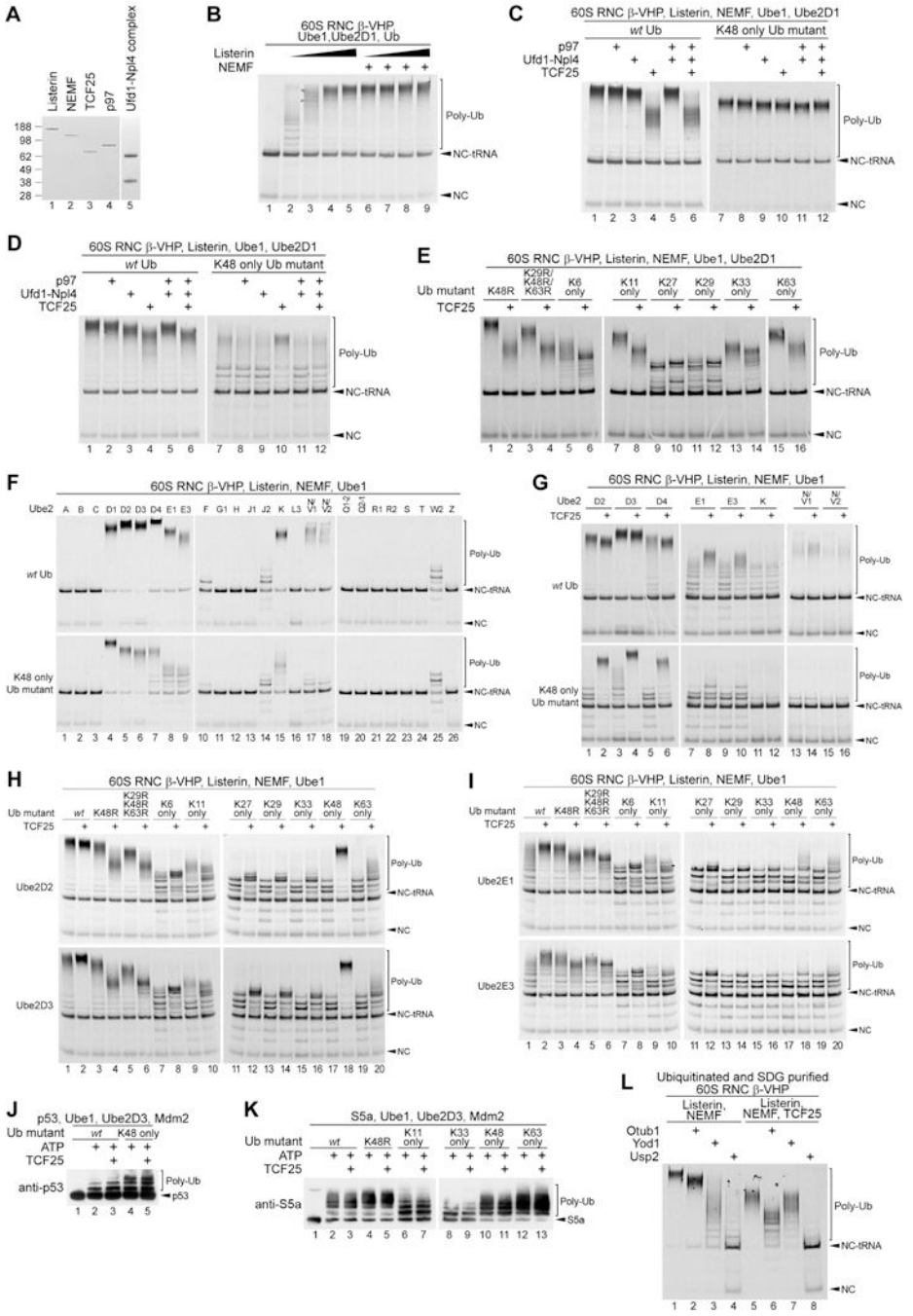

Figure 3. TCF25 imposes K48-specificity on Listerin-mediated ubiquitination of 60S RNCs

(A) Recombinant Listerin, NEMF, TCF25, p97 and Ufd1-Npl4. (B) Ubiquitination of β-VHP-containing 60S RNCs by Listerin (15–120 nM), Ube1 and Ube2D1 with *wt* Ub in the presence/absence of NEMF. (C-D) Influence of TCF25, p97 and Ufd1-Npl4 on ubiquitination of β-VHP-containing 60S RNCs by Ube1, Ube2D1 and (C) Listerin/NEMF or (D) Listerin with *wt* or K48 single-Lys mutant Ub. (E) Influence of TCF25 on ubiquitination of β-VHP-containing 60S RNCs by Listerin/NEMF, Ube1 and Ube2D1 with different Ub mutants. (F) Ubiquitination of β-VHP-containing 60S RNCs by Listerin/

NEMF, Ube1 and different Ube2 enzymes with *wt* or K48 single-Lys mutant Ub. (G) Influence of TCF25 on ubiquitination of β-VHP-containing 60S RNCs by Listerin/NEMF, Ube1 and different Ube2 enzymes with *wt* or K48 single-Lys mutant Ub. (H, I) Influence of TCF25 on ubiquitination of β-VHP-containing 60S RNCs by Listerin/NEMF, Ube1 and (H) Ube2D2/3 or (I) Ube2E1/3 with different Ub mutants. (J-K) Ubiquitination of (J) p53 or (K) S5a by Mdm2, Ube1 and Ube2D3 with *wt* or Ub mutants. (L) Activities of different deubiquitinating enzymes on SDG-purified Ub-β-VHP-containing 60S RNCs formed in the presence/absence of TCF25. (B-I, L) Ubiquitination was assayed by SDS-PAGE or (J-K) SDS-PAGE followed by western blotting. The positions of ubiquitinated products (Poly-Ub) are indicated on the right.

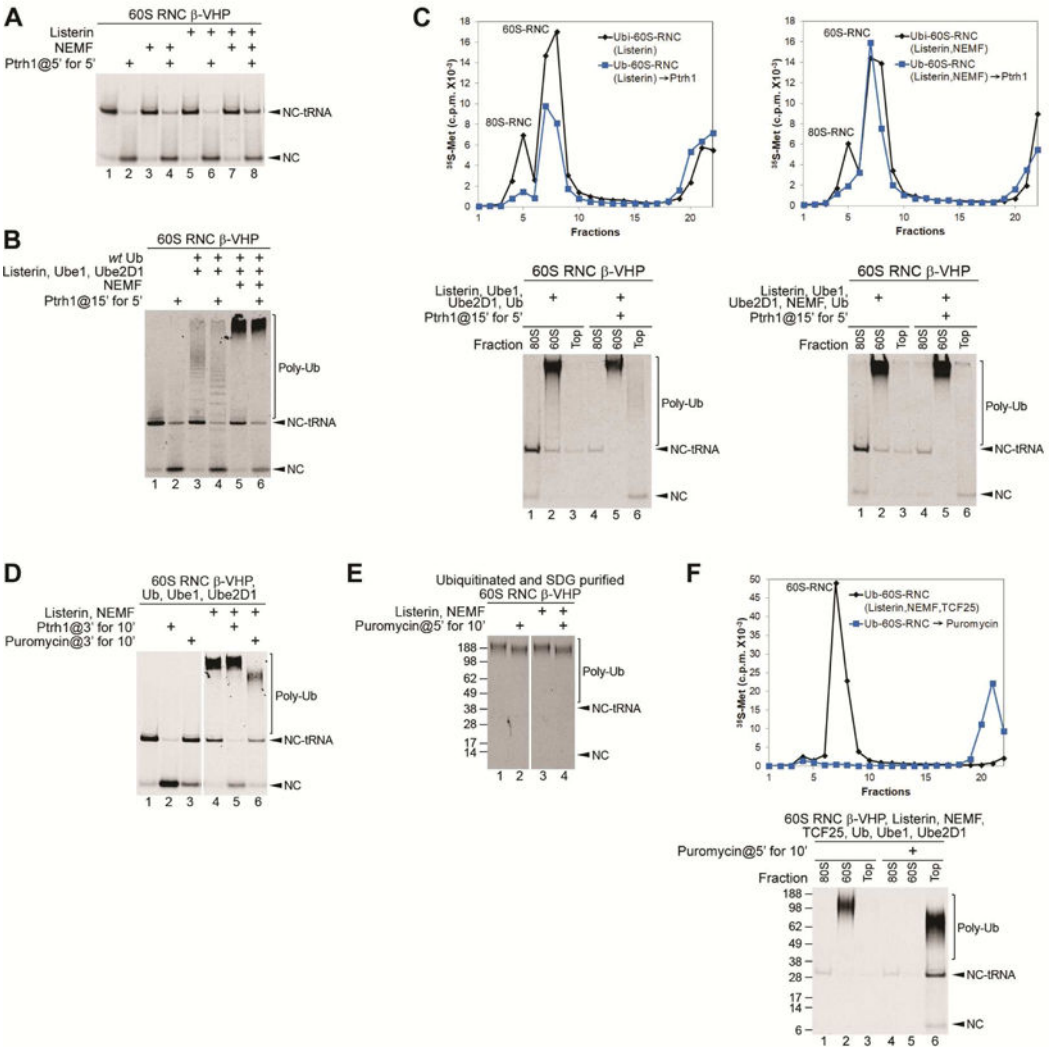

Figure 4. Release of ubiquitinated NCs from 60S RNCs is not promoted by Ptrh1, but can be induced by puromycin

(A) Influence of NEMF and Listerin on the activity of Ptrh1 on non-ubiquitinated 60S RNCs formed on β-VHP mRNA. (B) Influence of delayed addition of Ptrh1 on ubiquitination of 60S RNCs by Listerin, Ube1 and Ube2D1 with/without NEMF. (C) Influence of Ptrh1 on association of ubiquitinated NCs with 60S subunits upon its delayed addition to ubiquitination reactions containing 60S RNCs, Listerin, Ube1 and Ube2D1 with (right panels) or without (left panels) NEMF. (D) Influence of delayed addition of Ptrh1 and puromycin on ubiquitination of 60S RNCs by NEMF, Listerin, Ube1 and Ube2D1. (E) Influence of puromycin on SDG-purified ubiquitinated 60S RNCs. (F) Release of ubiquitinated NCs from 60S subunits by puromycin upon its delayed addition to ubiquitination reactions containing 60S RNCs, Listerin/NEMF, TCF25, Ube1 and Ube2D1. (A-B, D-E) Ubiquitination and release of NCs were monitored by SDS-PAGE or (C, F) by SDG centrifugation with subsequent analysis of fractions corresponding to RNCs and free NC/NC-tRNA by SDS-PAGE.

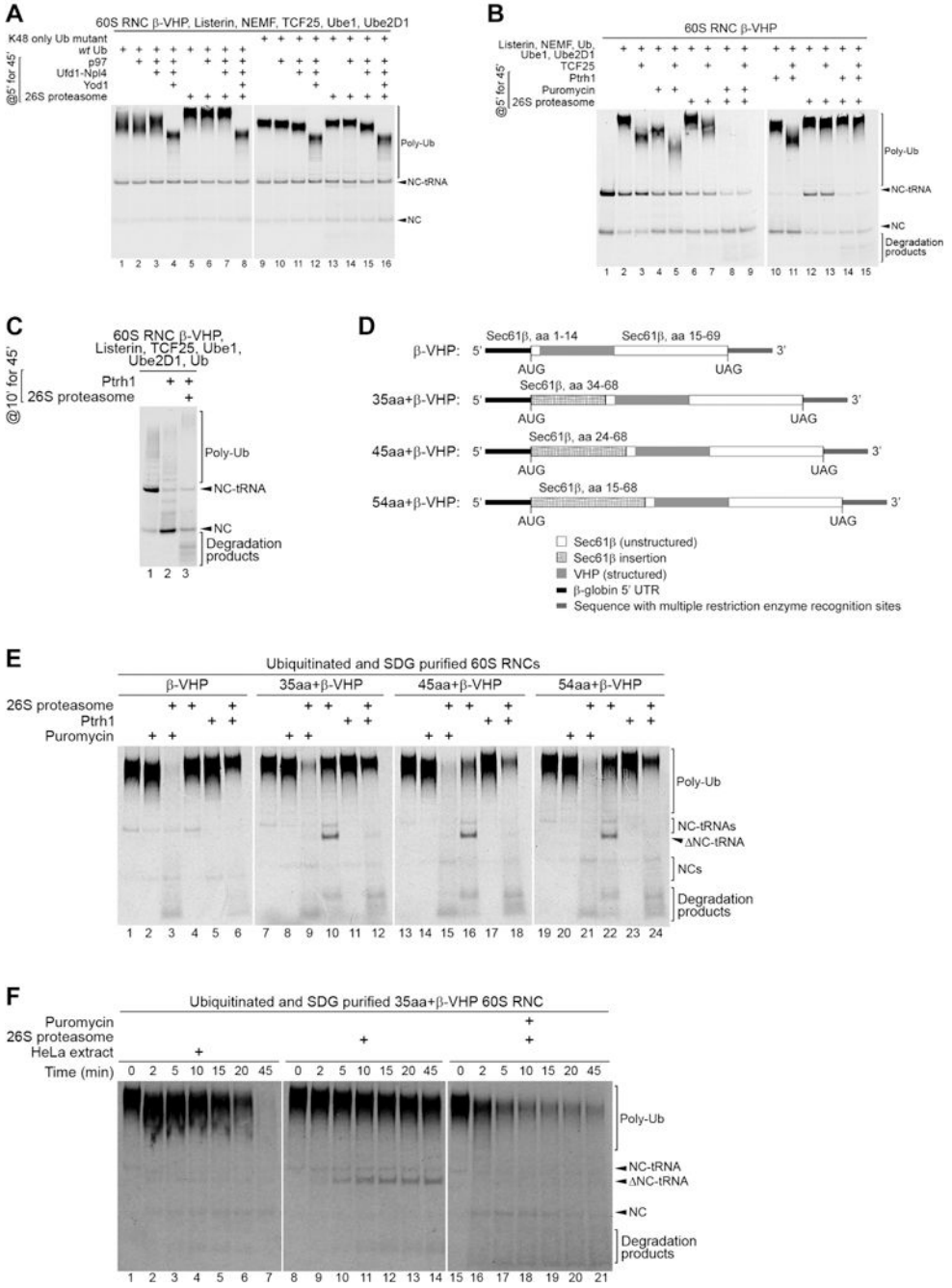

Figure 5. Proteasomal degradation of ubiquitinated NCs requires their release from 60S subunits

(A) Influence of 26S proteasome with/without p97, Ufd1-Npl4 and Yod1 on Ub-β-VHP-containing 60S RNCs obtained with Listerin/NEMF, TCF25, Ube1, Ube2D1 and *wt* or K48 mutant Ub. (B) Influence of 26S proteasome with/without puromycin or Ptrh1 on Ub-β-VHP-containing 60S RNCs obtained with Listerin/NEMF, Ube1, Ube2D1 and *wt* Ub in the presence/absence of TCF25. (C) Ptrh1-dependent 26S proteasomal degradation of Ub-β-VHP-containing 60S RNCs obtained in the absence of NEMF. (D) Schematic representation of β-VHP mutants containing unstructured N-terminal 35–54 aa-long extensions

corresponding to fragments of the C-terminal Sec61β region of β-VHP. (E) Proteasomal degradation of SDG-purified ubiquitinated 60S RNCs containing *wt* and N-terminally extended β-VHPs (Figure 5D) in the presence/absence of puromycin and Ptrh1. (F) Time courses of proteasomal degradation of SDG-purified ubiquitinated 60S RNCs containing N-terminally extended 35aa-β-VHP by HeLa cell extract and by 26S proteasome with/without puromycin. (A-C, E, F) Degradation of ubiquitinated NCs was assayed by SDS-PAGE.

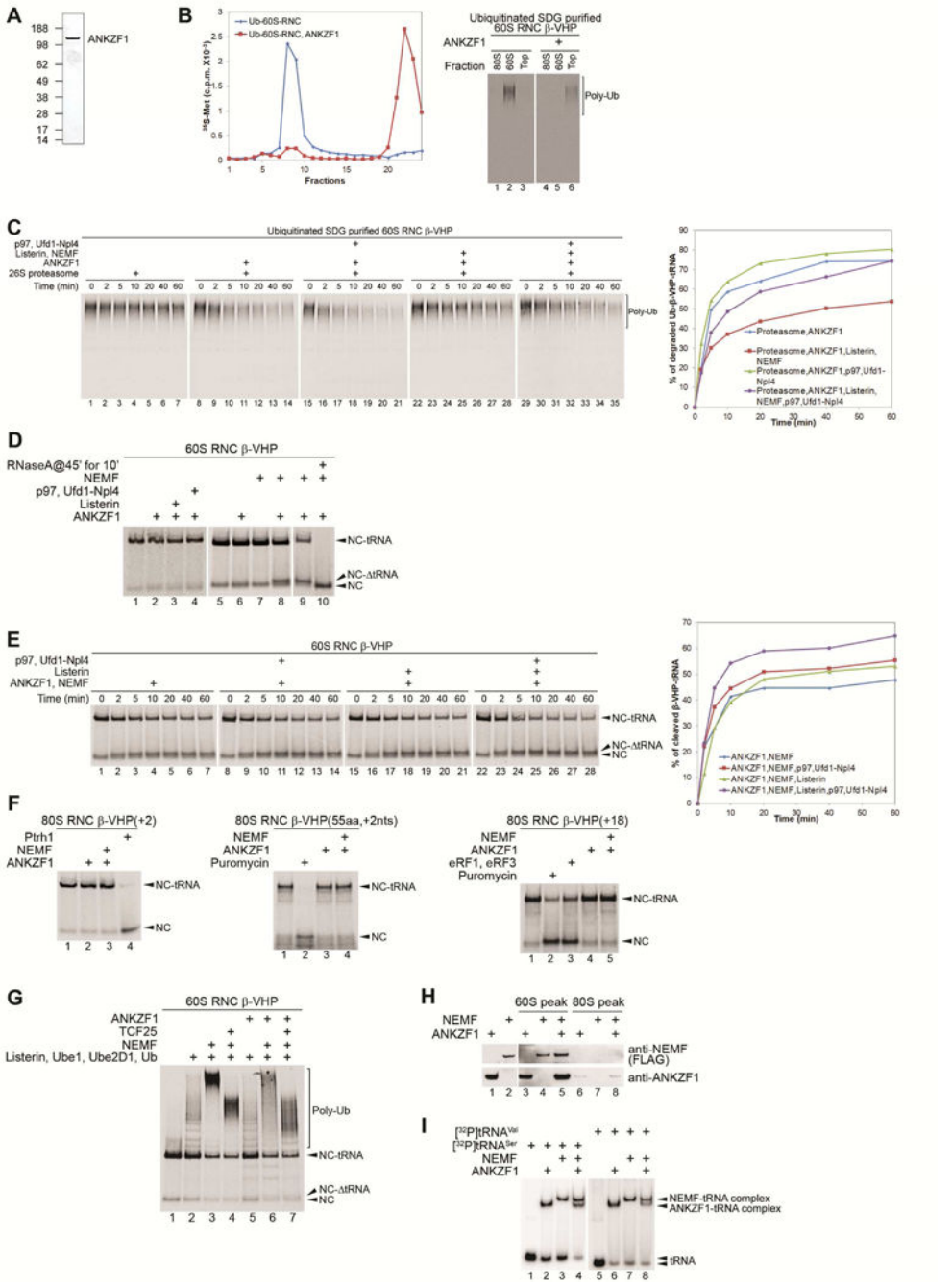

Figure 6. ANKZF1 promotes release of ubiquitinated NCs from 60S RNCs, allowing their proteasomal degradation

(A) Recombinant ANKZF1. (B) Release of Ub-β-VHP from SDG-purified ubiquitinated 60S RNCs by ANKZF1, assayed by SDG centrifugation (left panel) with subsequent analysis of fractions corresponding to RNCs and free NC/NC-tRNA by SDS-PAGE (right panel). (C) Representative time courses of ANKZF1-dependent 26S proteasomal degradation of Ub-β-VHP in SDG-purified ubiquitinated 60S RNCs in the presence/absence of Listerin/NEMF and p97/Ufd1-Npl4 (left panel) with subsequent quantification by Phosphorimager (right panel). (D) Release of β-VHP linked to a short $tRNA^{Val}$ fragment

from non-ubiquitinated 60S RNCs by ANKZF1 in the presence/absence of Listerin, p97/Ufd1-Npl4 and NEMF and its confirmation by delayed addition of RNase A, resulting in formation of free β-VHP. (E) Representative time courses of NEMF-dependent release of β-VHP-ΔtRNA^{Val} from non-ubiquitinated 60S RNCs by ANKZF1 in the presence/absence of Listerin and p97/Ufd1-Npl4 (left panel) with subsequent quantification by Phosphorimager (right panel). (F) The activity of ANKZF1 on 80S RNCs assembled on non-stop mRNAs encoding full-length or truncated (Figure 2E) β-VHP (two left panels) and on pre-termination complexes assembled on β-VHP mRNA containing 18 nt after the last sense codon (right panel). (G) The influence of ANKZF1 on ubiquitination of β-VHP-containing 60S RNCs by Ube1, Ube2D1 and Listerin in the presence/absence of NEMF and TCF25. (B-G) Ubiquitination and degradation of NCs were assayed by SDS-PAGE. (H) Association of ANKZF1 and NEMF with 60S subunits and 80S ribosomes, assayed by SDG centrifugation followed by western blotting. (I) Interaction of ANKZF1 and NEMF with [^{32}P]tRNA^{Ser} and [^{32}P]tRNA^{Val} assayed by EMSA.

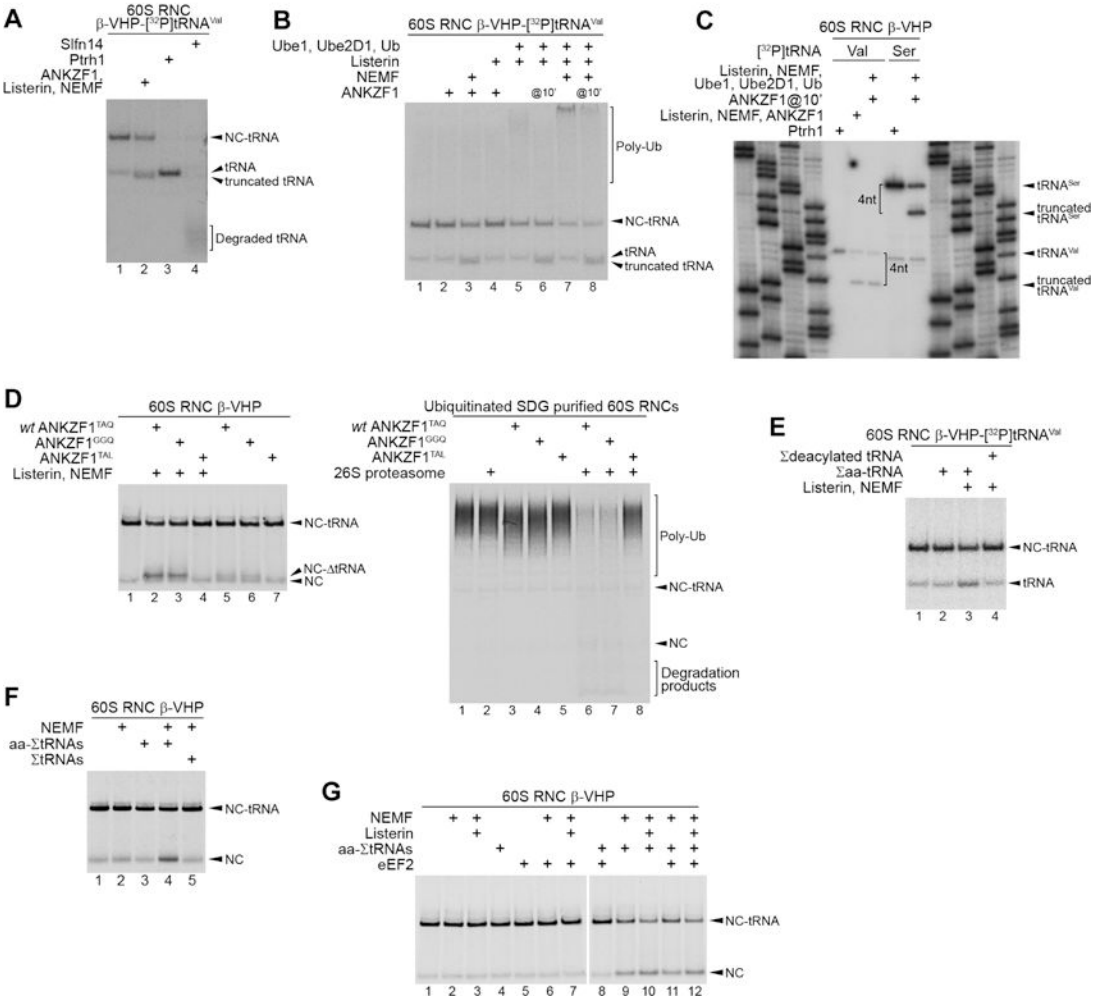

Figure 7. ANKZF1 releases NCs from 60S RNCs by inducing specific cleavage in the acceptor arm of the P site tRNA

(A) Comparison of the activities of ANKZF1, Ptrh1 and Slfn14 on 60S RNCs formed on β-VHP mRNA with Val-[^{32}P]tRNA^{Val}. (B) The activity of ANKZF1 on non-ubiquitinated and ubiquitinated 60S RNCs containing [^{32}P]tRNA^{Val}. (C) Determination of the site of cleavage in tRNA induced by ANKZF1 in ubiquitinated and non-ubiquitinated 60S RNCs containing [^{32}P]tRNA^{Val} or [^{32}P]tRNA^{Ser} assayed by sequencing gel electrophoresis. (D) Activities of TAQ$_{244–6}$→TAL and TAQ$_{244–6}$→GGQ ANKZF1 mutants in releasing β-VHP-ΔtRNA^{Val} from non-ubiquitinated 60S RNCs (left panel) and in stimulation of proteasomal degradation of Ub-β-VHP in SDG-purified ubiquitinated 60S RNCs (right panel). (E-G) The influence of Σ aminoacylated and deacylated tRNA on non-ubiquitinated 60S RNCs containing (E) β-VHP-[^{32}P]tRNA^{Val} or (F-G) [^{35}S]β-VHP-tRNA^{Val}, depending on the presence of NEMF, Listerin and eEF2. (A, B, D-G) Release and degradation of NCs were assayed by SDS-PAGE.